

Quantification of Uncertainty in Shale Gas Resources

AER/AGS Open File Report 2013-13

Quantification of Uncertainty in Shale Gas Resources

S. Lyster

Alberta Energy Regulator
Alberta Geological Survey

August 2013

©Her Majesty the Queen in Right of Alberta, 2013
ISBN 978-1-4601-0108-7

The Alberta Energy Regulator/Alberta Geological Survey (AER/AGS), its employees and contractors make no warranty, guarantee or representation, express or implied, or assume any legal liability regarding the correctness, accuracy, completeness or reliability of this publication. Any references to proprietary software and/or any use of proprietary data formats do not constitute endorsement by AER/AGS of any manufacturer's product.

If you use information from this publication in other publications or presentations, please acknowledge the AER/AGS. We recommend the following reference format:

Lyster, S. (2013): Quantification of uncertainty in shale gas resources; Alberta Energy Regulator, AER/AGS Open File Report 2013-13, 35 p.

Published August 2013 by:

Alberta Energy Regulator
Alberta Geological Survey
4th Floor, Twin Atria Building
4999 – 98th Avenue
Edmonton, AB T6B 2X3
Canada

Tel: 780.422.1927
Fax: 780.422.1918
E-mail: AGS-Info@aer.ca
Website: www.ags.gov.ab.ca

Contents

Acknowledgements.....	vi
Abstract.....	vii
1 Introduction.....	1
1.1 Introduction to Shale Gas.....	1
1.2 Resource Quantification and Uncertainty.....	1
1.3 Data Requirements.....	1
1.3.1 Geological Picks.....	2
1.3.2 Log Analysis.....	2
1.3.3 Isotherm Analysis.....	2
1.3.4 Mineralogy.....	3
1.3.5 Maturity Information.....	3
1.3.6 Reservoir Data.....	3
1.3.7 Dean Stark Analysis.....	3
1.4 Example Data.....	4
2 Mapping Spatial Variables.....	10
2.1 Gridding Methods.....	10
2.1.1 Detrending.....	10
2.1.2 Normal Score Transformation.....	10
2.1.3 Variography.....	10
2.1.4 Kriging.....	11
2.1.5 Back Transformations.....	11
2.2 Mapping Uncertainty – Estimation vs. Simulation.....	11
2.2.1 Local Uncertainty.....	12
2.2.2 Global Uncertainty.....	12
2.3 Upscaling.....	13
3 Calculating Dependent Variables.....	21
3.1 Linear Bivariate Relationships.....	21
3.2 Least-Squares Regression.....	21
3.3 Regression Uncertainty.....	21
3.4 Conditional Uncertainty.....	22
3.5 Bilinear Relationships.....	23
4 Determining Other Variables.....	25
4.1 Univariate Distributions.....	25
4.1.1 Water Saturation.....	25
4.1.2 Grain Density.....	26
5 Fluid Zones.....	27
5.1 Maturity Maps.....	27
5.2 Zone Cutoffs.....	27
5.3 Saturations and Coproduct Ratios.....	28
5.3.1 Linear Interpolation.....	28
5.3.2 Calculating Saturations.....	29
6 Resource Calculations.....	29
7 Simulation and Joint Uncertainty.....	30
8 Conclusions.....	30
9 References.....	34

Tables

Table 1. Variables used in the resource assessment methodology.	2
Table 2. Duvernay vitrinite reflectance (left) and hydrogen index (right).	28

Figures

Figure 1. The McKelvey box of the Petroleum Resources Management System.	4
Figure 2. A cross-section showing picks of the Duvernay Formation.	5
Figure 3. An example of a petrophysical log analysis.	6
Figure 4. An example of adsorption isotherm analysis results.	7
Figure 5. A thin section showing a long lens of vitrinite (V) in organic matter.	8
Figure 6. Dean Stark analysis results.	8
Figure 7. Data locations in the Duvernay Formation.	9
Figure 8. Kriging estimate map (left); simulated realization (right).	14
Figure 9. Net shale P10 (left); P90 (right).	15
Figure 10. Two realizations of depth to the top of the Duvernay Formation.	16
Figure 11. Two realizations of the net shale thickness of the Duvernay Formation.	17
Figure 12. Two realizations of the TOC content of the Duvernay Formation.	18
Figure 13. Two realizations of the shale porosity of the Duvernay Formation.	19
Figure 14. Example of upscaling.	20
Figure 15. Data showing the pressure vs. gas compressibility relationship in the basal Banff/Exshaw shale.	23
Figure 16. Data showing the uncertainty in the TOC-VL relationship in the Duvernay Formation.	24
Figure 17. Data showing the pressure vs. gas compressibility relationship in the basal Banff/Exshaw shale.	24
Figure 18. Histogram of water saturation, determined by Dean Stark analysis, in the Duvernay Formation.	26
Figure 19. Histogram of grain density in the Duvernay Formation.	27
Figure 20. Duvernay vitrinite reflectance (left) and hydrogen index (right).	31
Figure 21. Shale resource maps for the Duvernay Formation.	32
Figure 22. Conceptual diagram of the transfer function for the quantification of uncertainty in shale resources.	33

Acknowledgements

The methodology described in this report was developed as a part of the shale gas work done by the Energy Resource Appraisal Group of the Geology, Environmental Science, and Economics Branch of the Energy Resources Conservation Board. The author thanks the entire Energy Resource Appraisal shale gas project team: S.D.A. Anderson, A.P. Beaton, H. Berhane, T. Brazzoni, A. Budinski, D. Chen, Y. Cheng, T. Mack, C. Pana, J.G. Pawlowicz, and C.D. Rokosh. Thank you also to F.J. Hein for reviewing the report.

Abstract

Recent advances in fracturing and horizontal drilling technology have made unconventional petroleum resources increasingly important to the oil and gas industry in Alberta. The term ‘shale gas’ has largely become a catchall phrase to describe any unconventional plays that require fracturing, including shale gas, shale oil, tight gas, tight oil, and hybrid laminated reservoirs. With the emergence of these new sources of oil and gas, quantification of the resources has become a topic of major interest. The scarcity of historical data, sparse sampling of shale formations, and relatively poor understanding of unconventional reservoirs lead to large uncertainty in shale gas resource estimates. The Energy Resource Appraisal group of the Energy Resources Conservation Board has developed a methodology for quantifying the uncertainty in shale gas resource estimates in a geostatistical, data-driven framework that accounts for as many sources of uncertainty as possible.

1 Introduction

Recent technological developments—namely, horizontal drilling and hydraulic fracturing—have made extraction of hydrocarbons from low-permeability reservoirs technically and economically feasible. Unconventional reservoirs have been estimated by many organizations to contain massive amounts of hydrocarbons, dramatically increasing the worldwide resource base (Faraj et al., 2002; Faraj, 2005). The accessibility of these challenging new resources requires novel approaches to estimating total resource in place. This report outlines a methodology for modelling the resources in large, continuous, low-permeability reservoirs where there are few, if any, producing wells. The methodology is data driven and is built from the ground up to account for uncertainty at every step and in every variable.

1.1 Introduction to Shale Gas

Shale gas reservoirs are distinct from conventional hydrocarbon deposits in a number of ways: the shale acts as its own source, seal, and reservoir; the high organic content leads to oil and gas forming directly in the zones of interest; the low permeability traps a portion of the hydrocarbons; and the fabric of the shale contains both free hydrocarbons in pores and gas adsorbed to kerogen. These reservoirs are commonly referred to as shale gas but may include liquid hydrocarbon deposits (shale oil), low-permeability siltstone or sandstone formations (tight gas), and tight, organic-rich carbonate deposits. Many so-called shale gas deposits actually contain most of their hydrocarbons in interbedded silt and shale layers, or may not be true shale at all, but mudstone or siltstone.

These unique properties make it difficult to define pool boundaries, which is why shale gas is also referred to as a continuous petroleum resource (Schmoker, 2005). Other low-permeability reservoirs, such as ‘tight gas,’ are also termed continuous resources, and the methodology described here may apply to these resources as well.

1.2 Resource Quantification and Uncertainty

Shale gas resources are known for being exceptionally extensive compared to conventional hydrocarbon accumulations. This makes the distinction between reserves (technically recoverable and commercially viable) and resources (hydrocarbons in place) especially important because the recovery factor in unconventional pools is generally much lower than in conventional pools. The methodology focuses on calculating hydrocarbons initially in place, which is the largest and most all-encompassing category in the McKelvey box of the Petroleum Resources Management System (Figure 1 on page 4). This system is a set of definitions and a related classification system for petroleum reserves and resources that accounts for geology, current and future technology, and the growing importance of unconventional reservoirs (Society of Petroleum Evaluation Engineers, 2007). The methodology presented here was built to account for the left-to-right range of uncertainty in the McKelvey box, with every potential source of uncertainty taken into consideration to accurately quantify the uncertainty.

1.3 Data Requirements

A wide variety of data from a number of different sources are necessary to evaluate the resource potential of shale gas reservoirs due to particular properties of shale reservoirs.

Table 1 shows a list of the variables used in the methodology. The methodology presented here is data driven, with distributions and uncertainty being quantified from the available data and using as few assumptions and interpretations as possible.

Table 1. Variables used in the resource assessment methodology.

Variable	Abbreviation	Units	Data Source
Depth to top of shale unit	TOP	metres	Geological picks
Depth to base of shale unit	BASE	metres	
Gross thickness of shale unit (BASE–TOP)	GROSS	metres	
Thickness above specified gamma ray (GR) cutoff	NET	metres	Log analysis
Porosity of net shale	PHI	fraction or % by volume	
Total organic carbon content of net shale	TOC	% by weight	
Langmuir volume	VL	m ³ /g or m ³ /m ³	Isotherm analysis
Langmuir pressure	PL	kPa	
Grain density of shale	RHOG	g/cm ³	Mineralogy/XRD/XRF
Vitrinite reflectance	RO	% or fraction	Organic petrography
Hydrogen index	HI	mg/g	Rock Eval™
Temperature value of Rock Eval™ S2 peak	TMAX	Kelvin	
Pressure of reservoir at specified depth	PRES	kPa	
Temperature of reservoir at specified depth	TEMP	Kelvin	Reservoir data
Compressibility of gas	ZI	unitless	
Formation volume factor of oil	BOI	unitless	
Water saturation	SW	fraction or % by volume	Dean Stark analysis

1.3.1 Geological Picks

Expert geological interpretation of the top and base of geological strata builds the framework for the resource estimates. The depth to top, depth to base, and gross thickness of the shale unit represent the volume of rock that contains the hydrocarbons. Figure 2 shows an example of a cross-section with picks of the top and base of the Duvernay Formation (in addition to other markers).

1.3.2 Log Analysis

Log analysis is calibrated by measured lab data. The petrophysical properties that are determined by log analysis begin to characterize the volume that was constructed by the geological picks. Net shale thickness (from gamma-ray logs, for example), total porosity (from density, neutron, or sonic logs), and total organic carbon (from resistivity and sonic logs [Passey et al., 1990]) are the necessary parameters from this data source. Other reservoir properties, such as water saturation or mineralogy, may be determined from log analysis depending on what logs are available. Figure 3 shows an example of a comprehensive log analysis with numerous petrophysical properties derived from an assortment of geophysical logs.

1.3.3 Isotherm Analysis

The organic matter in shale that transforms into oil and gas also retains a portion of the methane (and other gases) through adsorption. As the pressure in the reservoir decreases through production, adsorbed gas is released, contributing to the ultimate recovery from wells. In our case, we used adsorbed gas

isotherms because, while preferable, desorbed gas isotherms were not available to us. To quantify the amount of adsorbed gas in shale, a Langmuir isotherm is used to model the relationship between pressure and adsorbed gas. The two parameters describing the shape of a Langmuir isotherm are the Langmuir volume (the ultimate potential for gas adsorption at infinite pressure) and the Langmuir pressure (the pressure at which half of the ultimate storage capacity is reached). These parameters are related to total organic carbon, and a number of isotherm analyses can be combined to quantify the relationship. Figure 4 shows an example of lab results for a Langmuir isotherm. Each data point corresponds to the recorded pressure at a stage of the adsorption analysis and the volume of methane adsorbed by the rock sample at that pressure. The line fit to the data points follows a Langmuir isotherm equation.

1.3.4 Mineralogy

Density logs are the primary source of porosity data for our analysis of shale gas. The bulk density is used to calculate porosity, given the fluid and grain density. For conventional reservoirs composed primarily of clean sandstone, for example, the lithology and grain density are quite well defined, and small variations have little effect on the calculated density-porosity, especially in highly porous rocks. Shale often contains more heavy minerals than sandstone and typically has lower porosity, so small variations in the grain density have a major impact on the calculated porosity. For these reasons, the mineralogy of a shale unit must be determined to quantify the porosity, and therefore free gas. The method we have used for mineralogy uses X-ray diffraction (XRD) and X-ray fluorescence (XRF) analyses.

1.3.5 Maturity Information

Shale formations can extend over huge areas, sometimes tens of thousands of square kilometres, hundreds of kilometres in one dimension. Over such large extents, the burial and thermal histories of the formation can vary significantly, meaning that there are different windows of maturity (from immature to mature to overmature), with the hydrocarbon content correspondingly varying from kerogen to heavy oil to light oil to condensate to gas. The primary indicator of maturity used in this workflow is vitrinite reflectance. Figure 5 shows a thin section with vitrinite in organic matter. Other indicators of thermal maturity, such as Rock Eval™ Tmax, could be used in a similar manner.

1.3.6 Reservoir Data

The amount of hydrocarbons contained in a reservoir depends on the size of the container (pore space), the conditions in the container, and the properties of the fluids being stored in that container. Pressure and temperature data from well tests, drillstem tests, or reservoir analogues are used to determine the relationship between depth, temperature, and pressure. Fluid properties such as gas compressibility and oil formation volume factor (or shrinkage) are determined from fluid tests or reservoir analogues. Direct measurements often indicate that shale reservoirs are over-pressured. In the early stage of appraisal, no direct data are available for the shale reservoirs themselves, so conventional pools that are thought to be in communication with the shale are used as an analogue. The data from nearby formations, when recalibrated, may result in pressure and temperature data that are near regional gradients, resulting in conservative estimates of resource endowment. This approach is not perfect and leads to significant uncertainty, but in the absence of sufficient direct measurements from the shale formations, it is an adequate substitute.

1.3.7 Dean Stark Analysis

The pore space in a shale reservoir is limited, and volume taken up by water cannot contain hydrocarbons. Water saturation is an important consideration in quantifying the resources. Dean Stark analysis provides

saturation information of core samples; however, the effectiveness of this test in quantifying the amount of water in shale, especially if using core from older wells, is uncertain. Nonetheless, Dean Stark analysis is the best direct measurement of water saturation that is available. Figure 6 shows an example of Dean Stark analysis results.

1.4 Example Data

The methodology used for estimating shale hydrocarbon resources with uncertainty is explained in the following sections. Examples for each step are shown where appropriate. The data used in the examples are from the Duvernay Formation unless otherwise noted. Figure 7 shows the locations of the data for the resource assessment of the Duvernay Formation (Rokosh et al., 2012).

Petroleum Initially in Place (PIIP)	Discovered PIIP	Commercial	Production		
			Reserves		
			Proved	Probable	Possible
		Sub-commercial	Contingent Resources		
			1C	2C	3C
			Unrecoverable		
	Undiscovered PIIP	Prospective Resources			
		Low	Best Estimate	High	
		Unrecoverable			

Figure 1. The McKelvey box of the Petroleum Resources Management System (Society of Petroleum Evaluation Engineers, 2007).

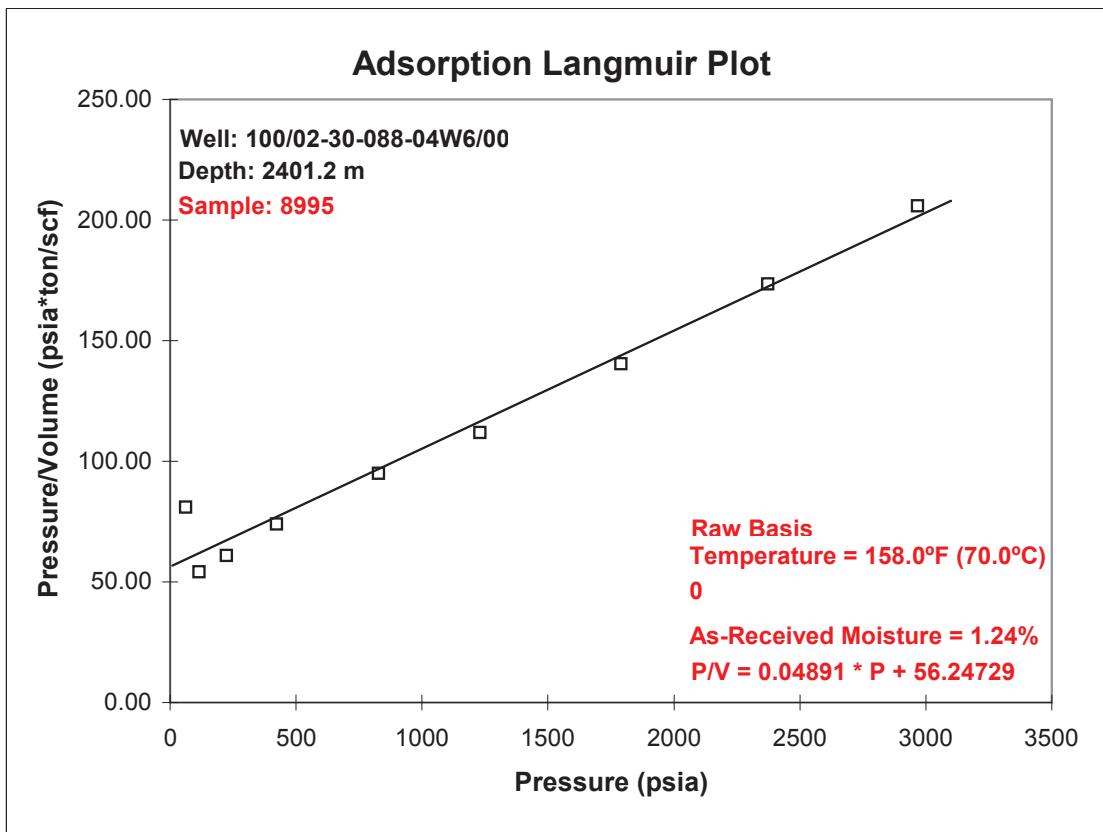
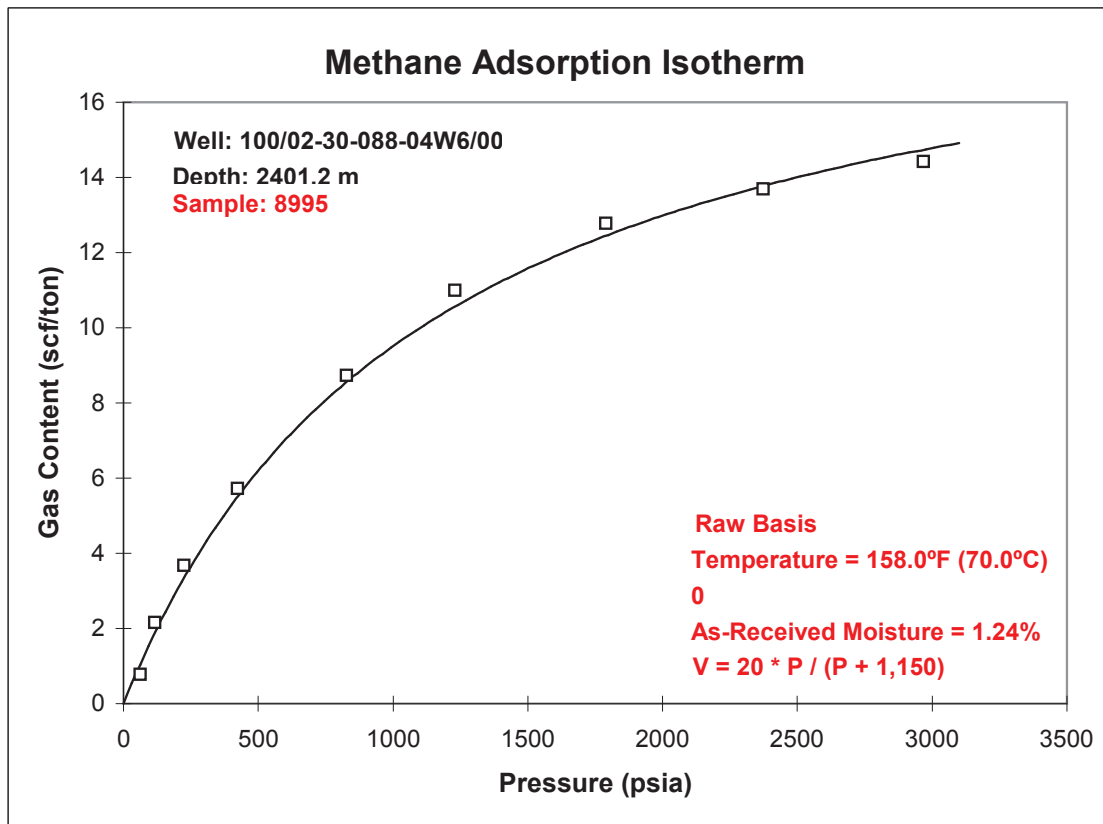


Figure 4. An example of adsorption isotherm analysis results (Beaton et al., 2010a).

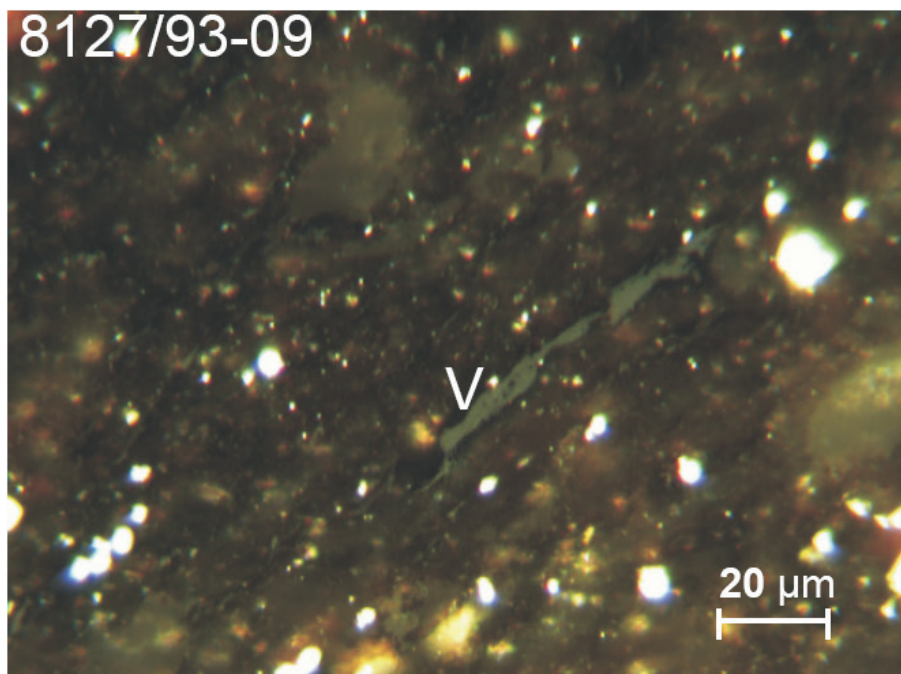


Figure 5. A thin section showing a long lens of vitrinite (V) in organic matter (Beaton et al., 2010b).

ERCB ID	Depth	Depth Unit	Well Location	Formation	As received			Dry & Dean Stark Extracted Conditions			
					Bulk Density (g/cc)	Gas-filled Porosity (%)	Gas Saturation (%)	Grain Density (g/cc)	Porosity (%)	Oil Saturation ⁽³⁾ (%)	Water Saturation ⁽⁴⁾ (%)
11851	2850.00	m	00/06-11-041-03W5	Duvernay	2.642	1.34	58.8	2.695	2.28	12.3	29.0
11853	7680.00	ft	00/16-18-052-05W5	Duvernay	2.685	0.11	17.0	2.698	0.65	57.3	25.7
11852	9464.90	ft	00/04-22-045-05W5	Duvernay	2.679	0.28	56.9	2.690	0.48	8.6	34.4
11863	1178.80	m	02/11-10-020-13W4/0	Exshaw	2.565	6.34	80.9	2.768	7.84	2.7	16.4
11864	1187.70	m	02/11-10-020-13W4/1	Exshaw	2.282	5.60	69.8	2.456	8.02	8.7	21.4
11868	1946.50	m	00/11-36-007-23W4/0	Exshaw	2.225	0.14	4.0	2.275	3.38	79.5	16.5
11869	1948.80	m	00/11-36-007-23W4/0	Exshaw	2.667	2.17	53.9	2.763	4.02	37.8	8.3
11865	6989.00	ft	00/14-29-048-06W5/0	Exshaw	2.541	0.15	13.0	2.561	1.12	58.3	28.7
11870	1266.20	m	00/14-18-058-03W5/0	Exshaw	2.691	3.40	53.2	2.843	6.40	4.9	41.9
11873	2349.50	m	00/03-05-081-06W6/0	Exshaw	2.667	0.42	24.1	2.702	1.76	19.0	56.9
11874	10231.00	ft	00/07-03-031-04W5/0	Exshaw	2.547	3.60	69.7	2.669	5.16	5.5	24.8
11876	8775.00	ft	00/04-12-015-27W4/0	Exshaw	2.506	0.17	11.3	2.532	1.55	27.7	61.0
11883	2016.00	m	00/16-07-077-25W5/0	Exshaw	2.336	0.20	8.6	2.373	2.32	78.7	12.7

Figure 6. Dean Stark analysis results (Rokosh et al., 2013b).

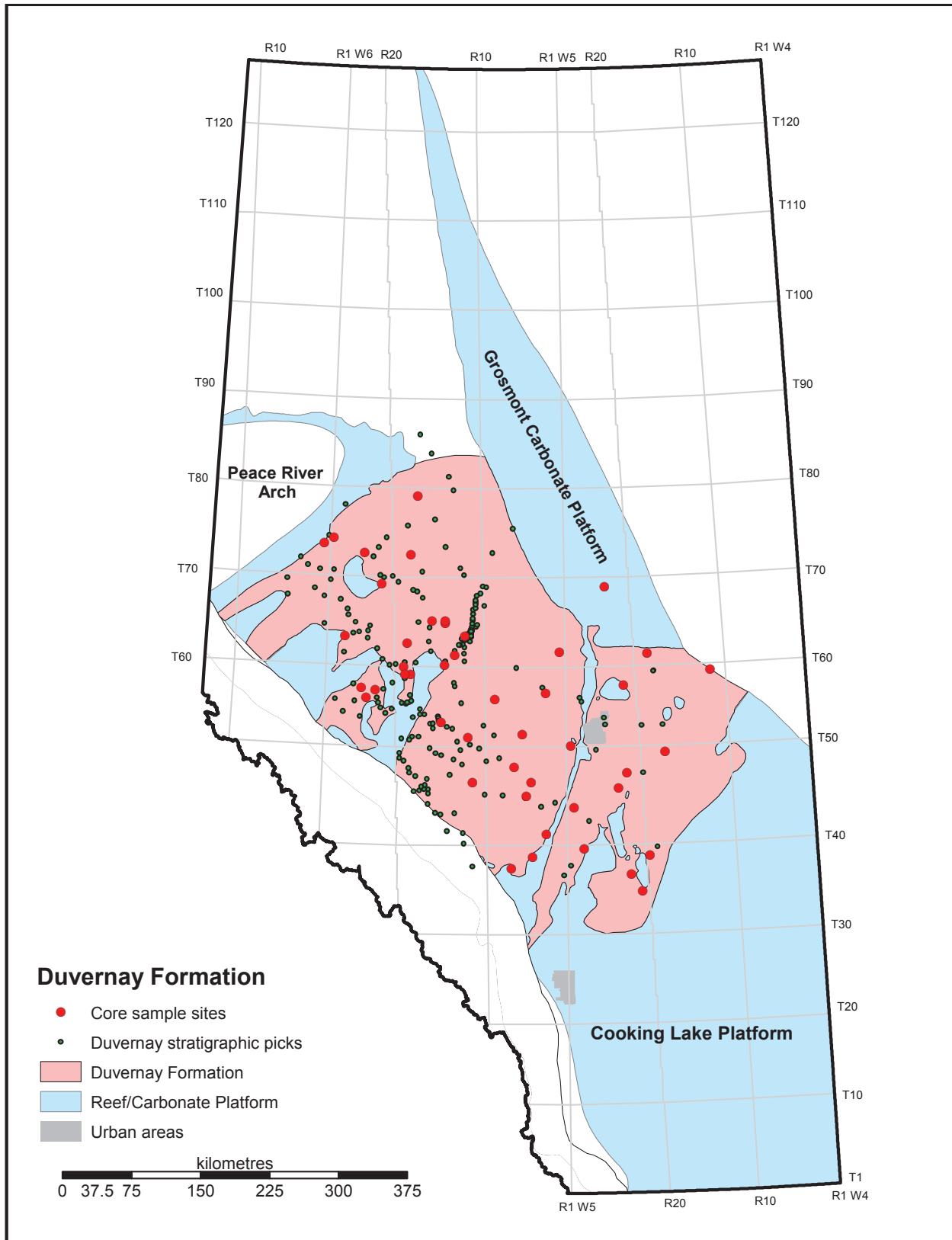


Figure 7. Data locations in the Duvernay Formation (Rokosh et al., 2012).

2 Mapping Spatial Variables

The first step in this methodology is to map the variables that have sufficient data density. The meaning of ‘sufficient’ data density is relative and varies based on the spatial structure of the shale being studied, the quality of the data, and the person doing the resource analysis. Typically those variables that come from geological picks or log analyses are considered spatial because gaps in the data can be filled by applying mapping or gridding methods. These variables are TOP, BASE, GROSS, NET, PHI, and TOC from Table 1. The TOP, BASE, and GROSS are redundant with one another and so do not all need to be explicitly modelled.

2.1 Gridding Methods

To represent a property with a grid that can account for uncertainty, geostatistical methods must be used. The workflow for creating a map of geological properties is presented in this section.

2.1.1 Detrending

Several of the variables used for shale gas resource calculations are not static over large study areas. Shale formations can be very extensive, stretching hundreds of kilometres. Because of this, some variables need to be decomposed into a systematic trend and locally varying residuals:

$$R(u) = Z(u) - m(u) \quad (1)$$

where $R(u)$ is the residual value, $Z(u)$ is the variable value, and $m(u)$ is the mean (or trend) value at location u . The residual is then modelled and added back to the trend at the end of the workflow. Residuals are in the same units as the original variable as they are local-scale deviations from the large-scale trend.

2.1.2 Normal Score Transformation

A normal score transformation is applied to a variable (or residual) to ensure its mathematical properties. When a back transformation is subsequently applied, a nonparametric local distribution can be determined. A normal score transform is applied quantile by quantile as follows:

$$y = G^{-1}(F(z)) \quad (2)$$

where y is the transformed normal value, G^{-1} is the inverse standard normal cumulative function, F is the cumulative input distribution, and z is the value being transformed. So the original variable is converted to a cumulative quantile distribution, then the equivalent standard normal value is found for that quantile. The transformed normal variable y is unitless, or is sometimes said to be in normal score units.

2.1.3 Variography

The spatial structure of a variable must be quantified mathematically to calculate estimates and uncertainty. The standard method for accomplishing this is variography, or variogram calculation and modelling. The equation for a variogram of variable $Y(u)$ is

$$\gamma(h) = \frac{E\{[Y(u) - Y(u+h)]^2\}}{2} \quad (3)$$

where γ is the variogram value and h is the lag distance or separation vector. Once the variogram is calculated, a model function is fit to ensure the positive definiteness of the kriging system of equations.

2.1.4 Kriging

Kriging is a linear estimator that determines the optimal estimate for a value at a given location based on the closeness and redundancy of the surrounding sampled data points. The general equation for a linear estimate is

$$Y^*(u) = \sum_{i=1}^n \lambda_i \cdot Y(u_i) \quad (4)$$

where $Y^*(u)$ is the estimated value of Y at location u , λ_i is the weight assigned to the i th nearby data value at location u_i , and $Y(u_i)$ is the known data value at location u_i , out of n locations used to make the estimate. The difference between linear estimation methods is in how the weights are assigned. Kriging uses an n -by- n system of equations that minimizes the error variance:

$$\sum_{j=1}^n Cov\{u_i, u_j\} \cdot \lambda_j = Cov\{u, u_i\} \quad \forall i = 1, \dots, n \quad (5)$$

where $Cov\{u_i, u_j\}$ is the covariance between locations u_i and u_j (each pair of known data values) and $Cov\{u, u_i\}$ is the covariance between the location to be estimated, u , and the known data location u_i . The covariance values are determined from the modelled variogram using the equation

$$Cov(h) = \sigma_Y^2 - \gamma(h) \quad (6)$$

where $Cov(h)$ is the covariance between two locations separated by lag distance h and σ_Y^2 is the variance of Y (which is equal to 1 if Y is a normalized variable).

2.1.5 Back Transformations

Once the kriging estimates have been determined, the original variable estimate is determined by reversing the normal score transform and then adding the trend back to the residual. The normal score transformation is reversed to determine the estimated residual by the equation

$$R^*(u) = F^{-1}(G(Y^*(u))) \quad (7)$$

where $R^*(u)$ is the estimate of the residual, F^{-1} is the inverse of the input cumulative distribution, and G is the standard normal cumulative function. The residual estimate is added to the trend (mean) value at each location:

$$Z^*(u) = R^*(u) + m(u) \quad (8)$$

where $Z^*(u)$ is the kriging estimate of the original variable, Z , at location u .

2.2 Mapping Uncertainty – Estimation vs. Simulation

The kriging estimates for each spatial variable create maps that are useful for illustrating areas of particular interest. However, they are not appropriate for quantifying uncertainty in resource estimates because kriging, like any interpolation method, produces maps that are too smooth. Simulation is needed to create maps that reflect the variability inherent in real geological variables. Figure 8 on page 14 shows a map of kriging estimates and a simulated realization for the net shale thickness of the Duvernay Formation.

The simulated map clearly has much more variability than the overly-smooth kriged map. However, a geostatistical simulation is not unique and is used to generate a number of maps, all equally probable.

These different maps represent the range of uncertainty in the variable over the whole study area. In this context, kriging is used to calculate local uncertainty, and simulation is used to quantify global uncertainty.

2.2.1 Local Uncertainty

Local uncertainty refers to the distribution of possible outcomes at a specified location. Kriging is used to determine the local uncertainty. The variance of the kriging estimate (also called kriging variance) is calculated by the equation

$$\sigma_{Y^*(u)}^2 = 1 - \sum_{i=1}^n \lambda_i \cdot Cov\{u, u_i\} \quad (9)$$

where the terms are as defined in Equations 4 and 6. The square root of the kriging variance, also called the kriging standard deviation or standard error, defines the width of the normal distribution of uncertainty in normal score units. This local distribution of uncertainty is only valid at location u . To determine the local uncertainty in the original variable units, a quantile-to-quantile back transformation is performed and the local trend value is added:

$$Z^{P10}(u) = F^{-1}\left(G\left(Y^*(u) - 1.28 \cdot \sigma_{Y^*(u)}\right)\right) + m(u) \quad (10)$$

where Z^{P10} is the P10 (tenth percentile, low) value of the local uncertainty distribution and 1.28 is the number of standard deviations from the mean for the tenth percentile of a normal distribution. The other terms are as defined above in Equations 1 and 2. The P90 (ninetieth percentile, high) value is found by back transforming the ninetieth percentile of the local normal distribution:

$$Z^{P90}(u) = F^{-1}\left(G\left(Y^*(u) + 1.28 \cdot \sigma_{Y^*(u)}\right)\right) + m(u) \quad (11)$$

Any quantile that is desired could be calculated in this way, although the P10 and P90 are typically used to summarize the local uncertainty. Note that the P50 or median is the same as the kriging estimate, because in normal score units the mean and median are equal. Figure 9 shows maps of the P10 and P90 values for the net shale thickness in the Duvernay Formation. These maps represent low-case and high-case values for all locations; in reality, it is expected that 10% of the study area would have true shale thicknesses less than the P10 and 10% above the P90.

2.2.2 Global Uncertainty

The uncertainty in a variable over an entire study area is called global uncertainty. This is the joint distribution of the local uncertainty distributions at all locations simultaneously. These locations, considered together, do not follow the standard statistical assumptions of IID (independent and identically distributed). They are not independent, as shown by a variogram that is not pure noise. They are not identically distributed, as there are high and low areas in a map produced by kriging or another method, and local uncertainty distributions are not the same everywhere.

The joint distribution is of the order of N_{xyz} , the total number of locations contained in the study area (the number of grid cells in a map). As this can be on the order of millions, the distribution is far too complex to solve for analytically. Geostatistical simulation is used to sample from the joint distribution. To perform simulation, the local distributions are randomly sampled:

$$Y^{sim}(u) \sim N\left(Y^*(u), \sigma_{Y^*(u)}^2\right) \quad (12)$$

where $Y^{sim}(u)$ is the simulated value of Y at location u and the other variables are as defined in Equations 4 and 9. The original-units variable is then found via back transformation:

$$Z^{sim}(u) = F^{-1}\left(G\left(Y^{sim}\right)\right) + m(u) \quad (13)$$

where $Z^{sim}(u)$ is the simulated value of the original variable Z at location u .

The key to the simulation is that the Y^{sim} values at different locations are correlated to one another as defined by the variogram. This can be done either sequentially, where each Y^{sim} is used as conditioning data for the remaining Y^{sim} values (Deutsch, 2002), through a p-field type simulation where the Y^{sim} values are correlated before the back transformations are performed (Goovaerts, 1997), or by a process called “conditioning by kriging” (Chiles and Delfiner, 2012). This creates one possible realization of what the reality could be, based on the input data and the inferred variogram structure. By repeating this process many times (at least 10–20, but more typically 100), a number of realizations are generated, with each realization being a sample from the joint distribution of the spatial variable.

Figure 10 shows two realizations of the depth to the top of the Duvernay Formation; Figure 11 shows two realizations of the net shale thickness of the Duvernay Formation; Figure 12 shows two realizations of the TOC content of the Duvernay Formation; and Figure 13 shows two realizations of the shale porosity of the Duvernay Formation.

- The depth maps are dominated by the large-scale trend (see Equation 1) as the Duvernay Formation dips southwest towards the Rocky Mountains. Local fluctuations are significant but hard to see due to the use of one colour scale covering the whole area.
- The net shale maps always show thick shale in the centre-southwest area, but are very random towards the eastern part of the Duvernay Formation because there is significantly less data in that area.
- The TOC content has similar spatial structure as the net shale thickness but has less relative variability between the high and low values.
- The porosity of net shale has short-scale spatial correlation and is relatively random compared to the other spatial variables.

2.3 Upscaling

Once maps are generated for the spatial variables, the scale must be aligned with the units for resource calculation. In the ERCB shale evaluation (Rokosh et al., 2012), the maps were created with 400 m grid cells, which is the approximate size of a legal subdivision (LSD) in the Alberta Township System (ATS). The resources were calculated on a section-by-section basis, with a section in the ATS being one mile square, roughly 1600 m by 1600 m. The resource maps presented in Rokosh et al. (2012) show shale- and siltstone-hosted hydrocarbons aggregated to the township scale—one ATS township being six sections by six sections except near meridians or correction lines (McKercher and Wolfe, 1986). The aggregation of the simulated realizations from LSD scale to section scale also changes the local properties by reducing the variance to correspond to the increase in volume (Journel and Huijbregts, 1978). Figure 14 shows an example of the concept of upscaling. The dots correspond to the centroids of LSDs in a given area at approximately 400 m spacing. The squares are the outlines of sections, so most sections contain sixteen LSDs. The dark line is the erosional edge of the shale formation under consideration.

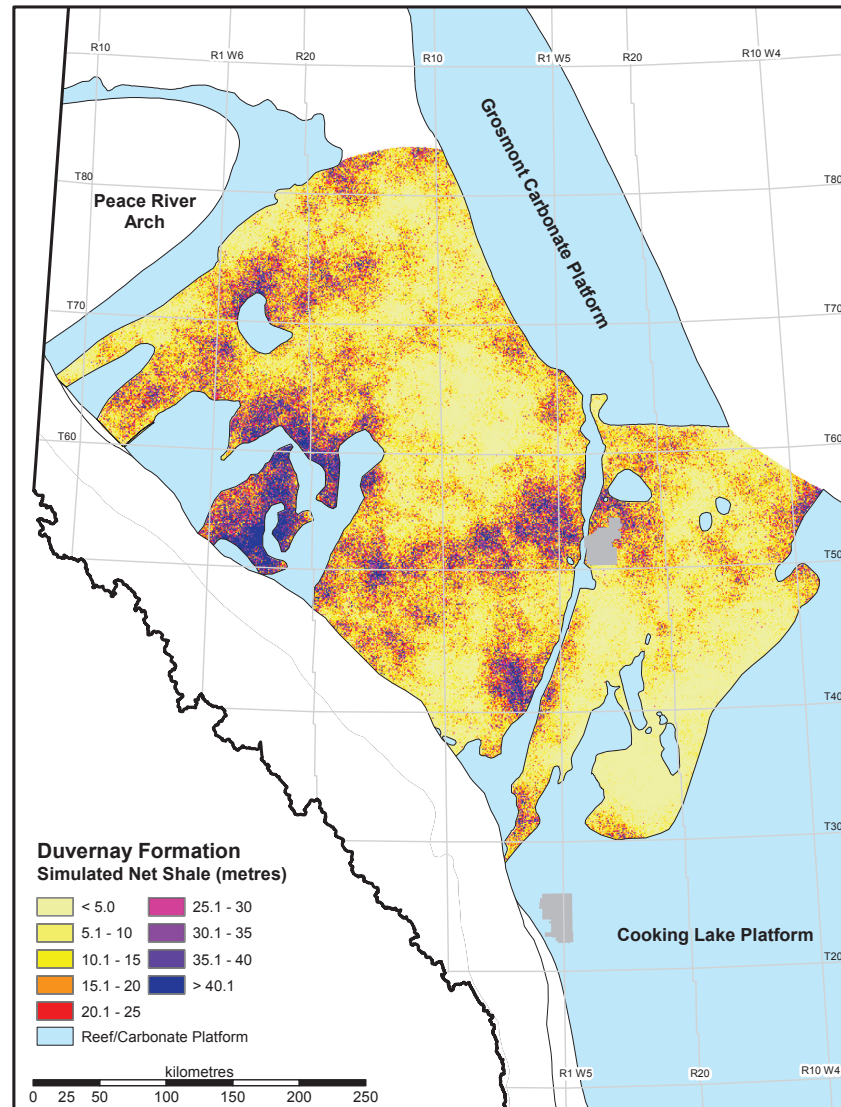
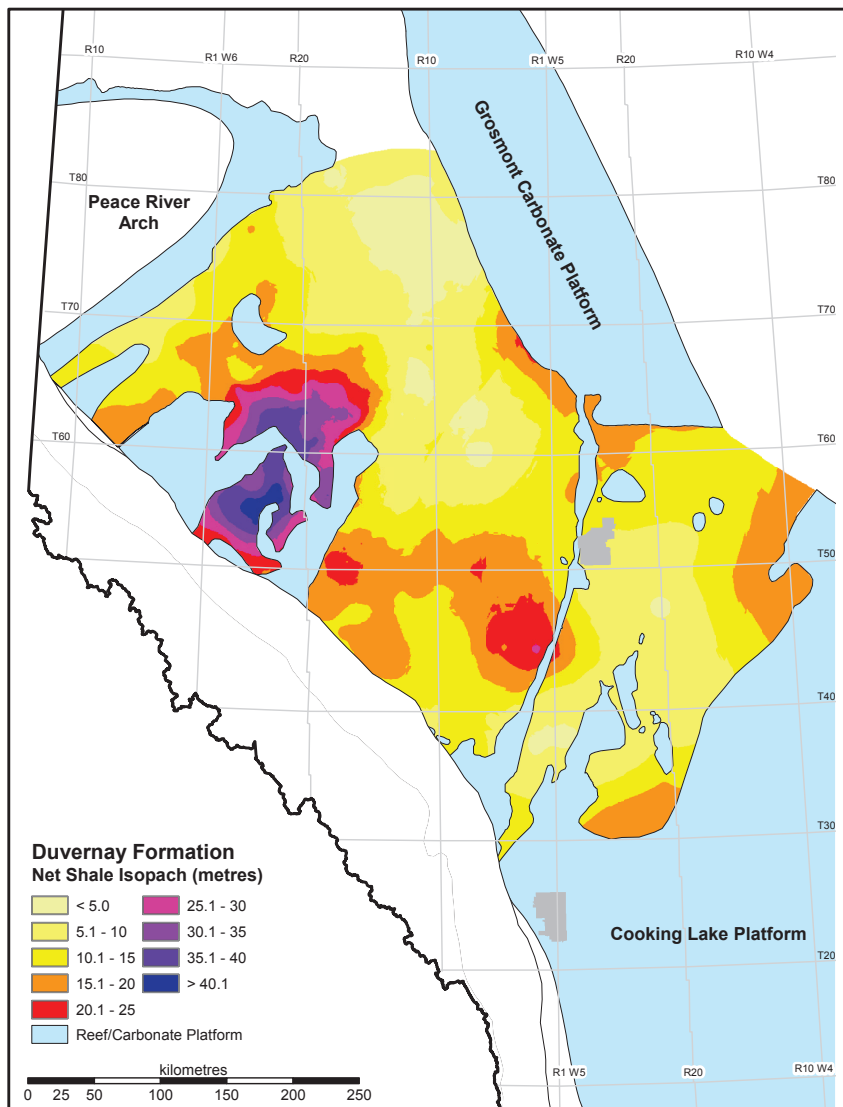


Figure 8. Kriging estimate map (left); simulated realization (right).

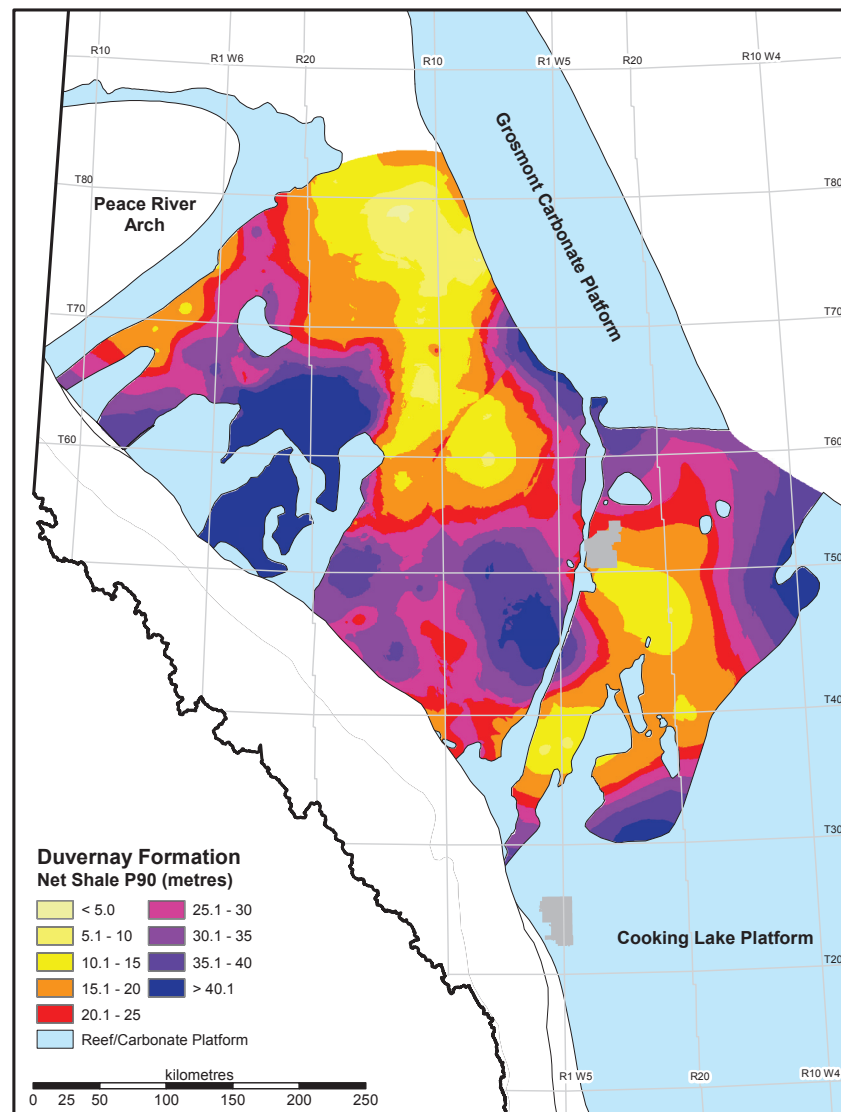
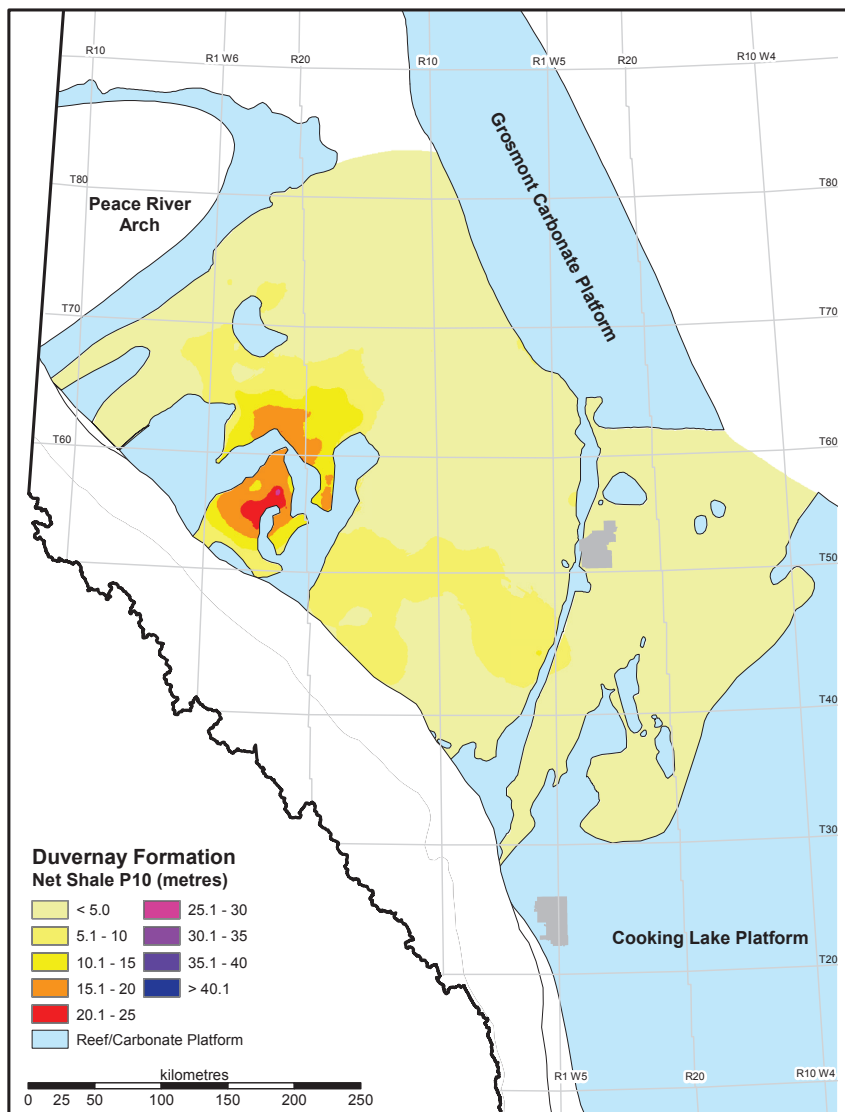


Figure 9. Net shale P10 (left); P90 (right).

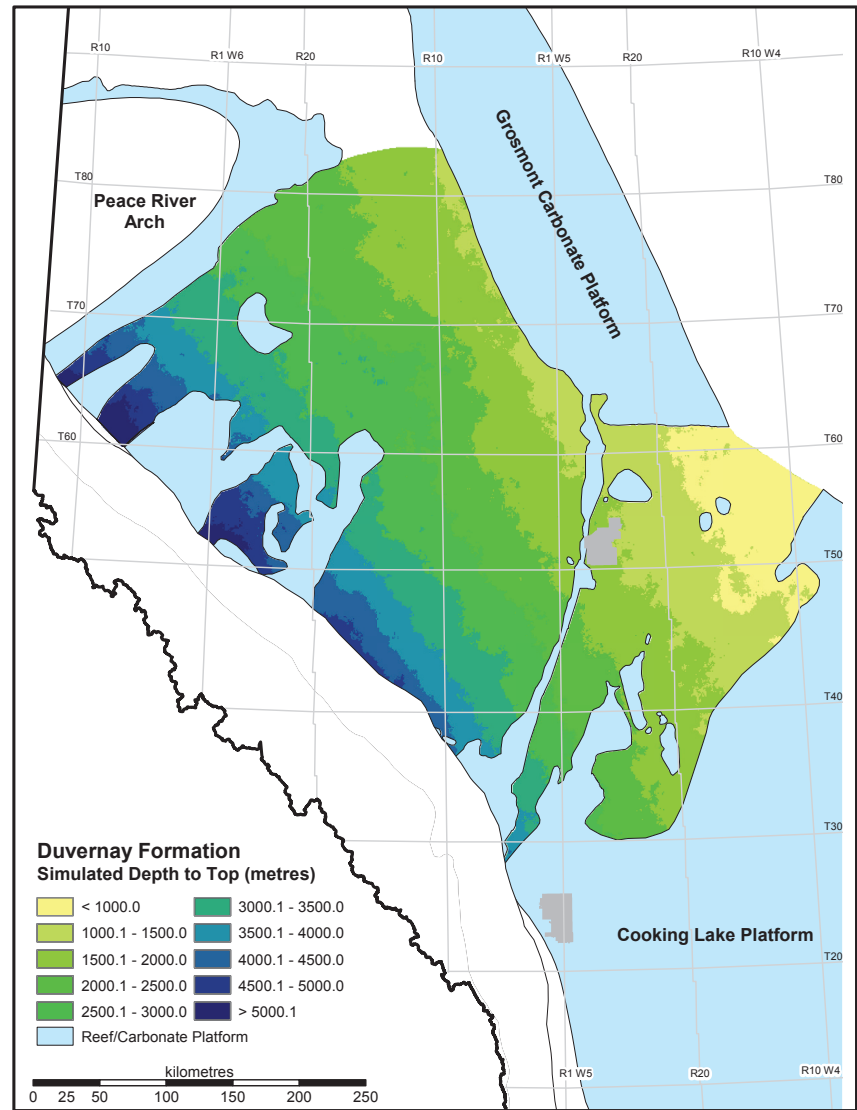
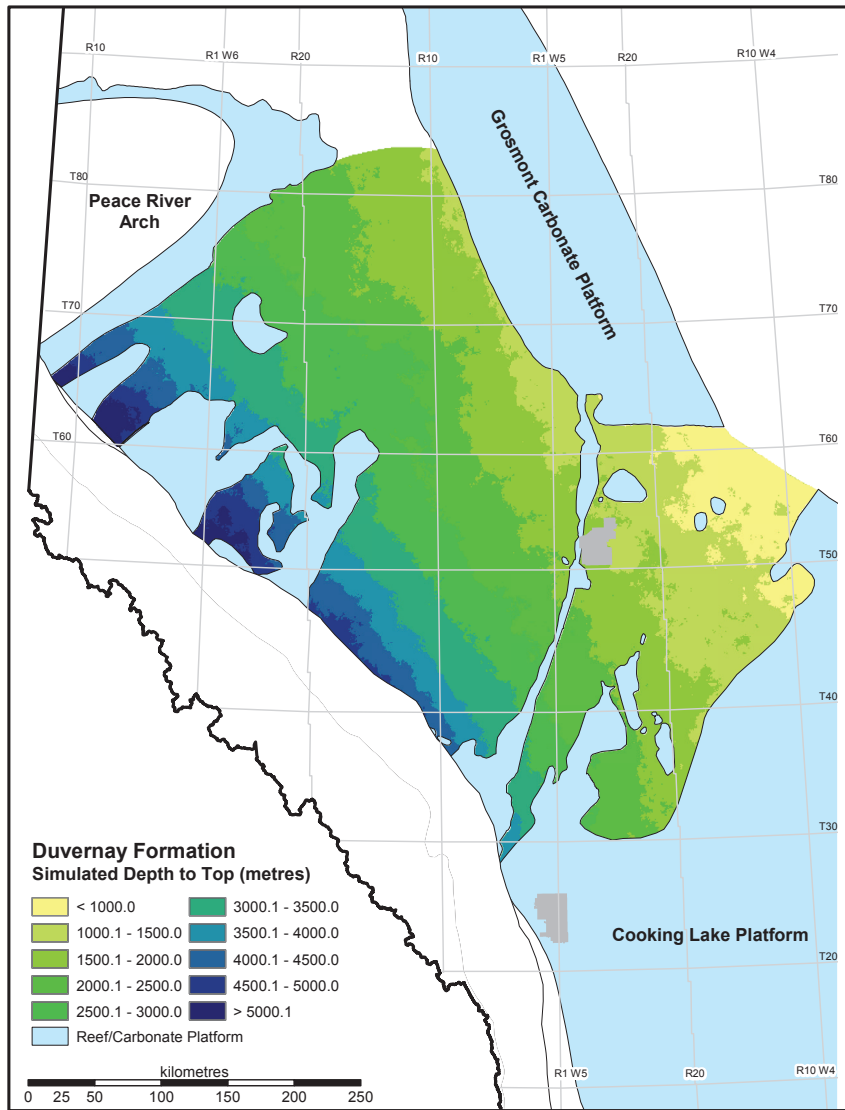


Figure 10. Two realizations of depth to the top of the Duvernay Formation.

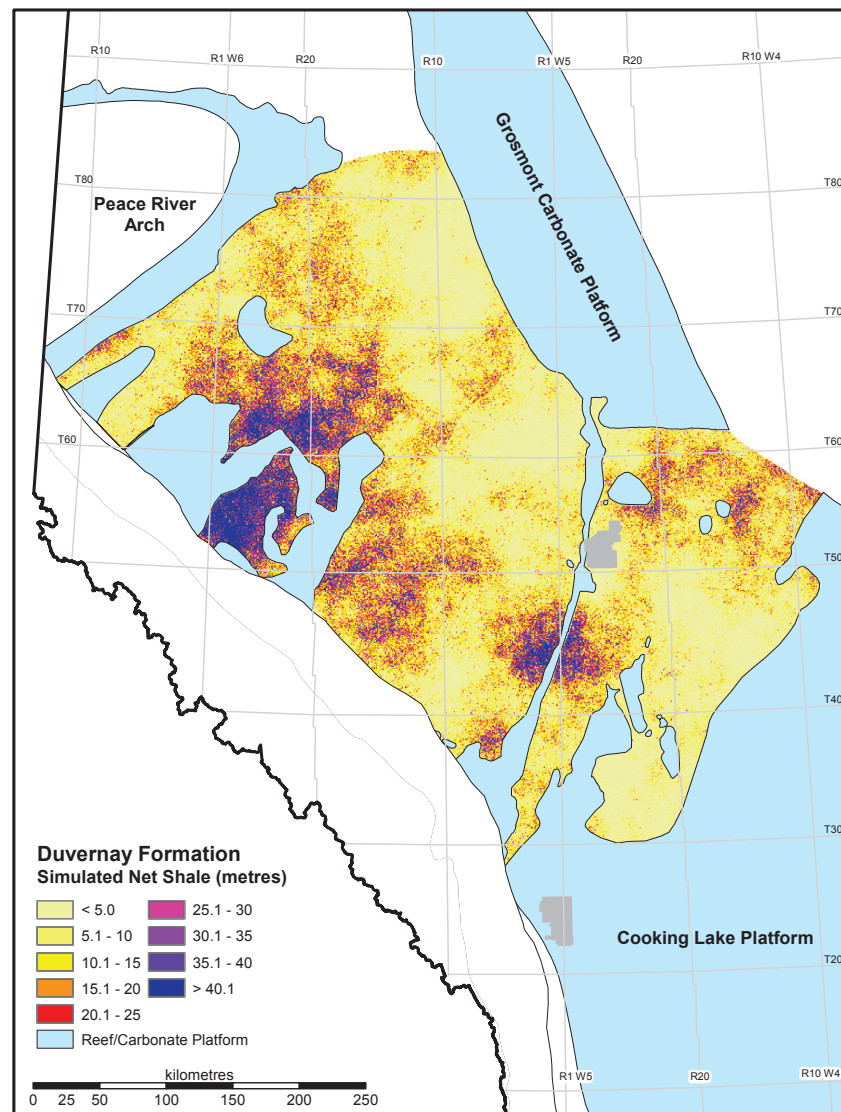
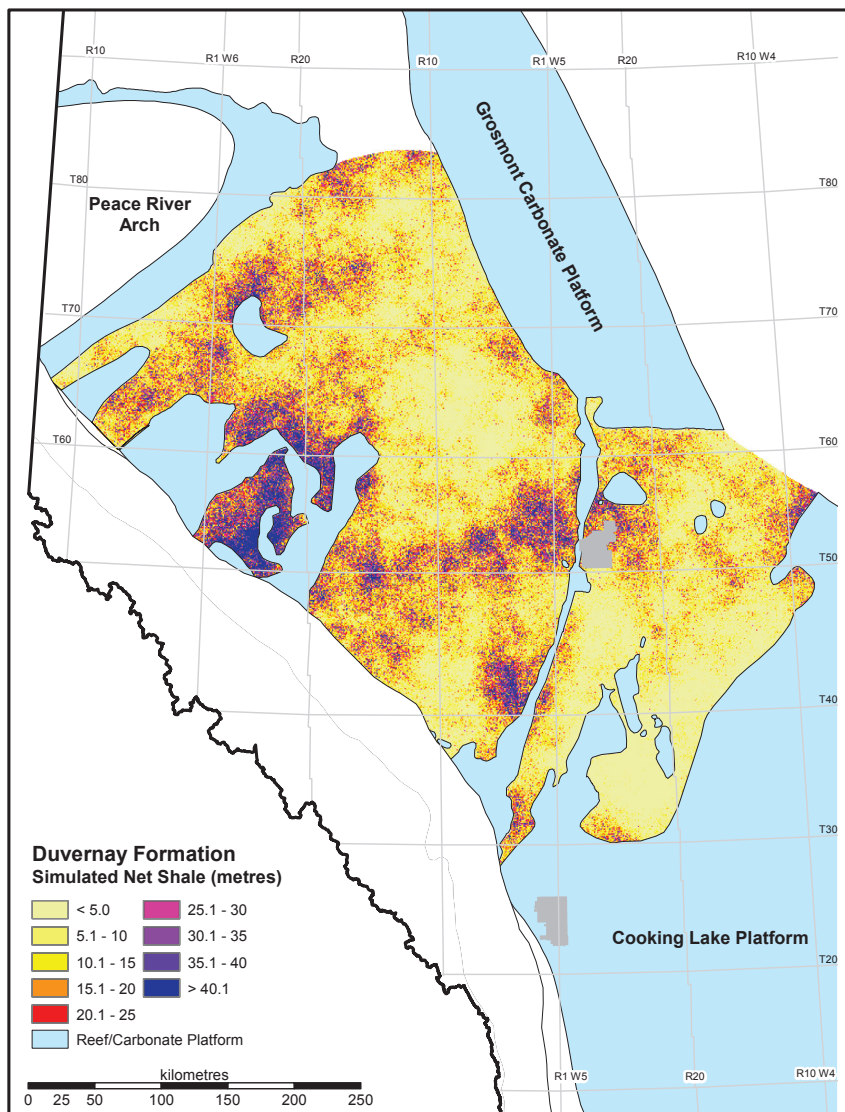


Figure 11. Two realizations of the net shale thickness of the Duvernay Formation.

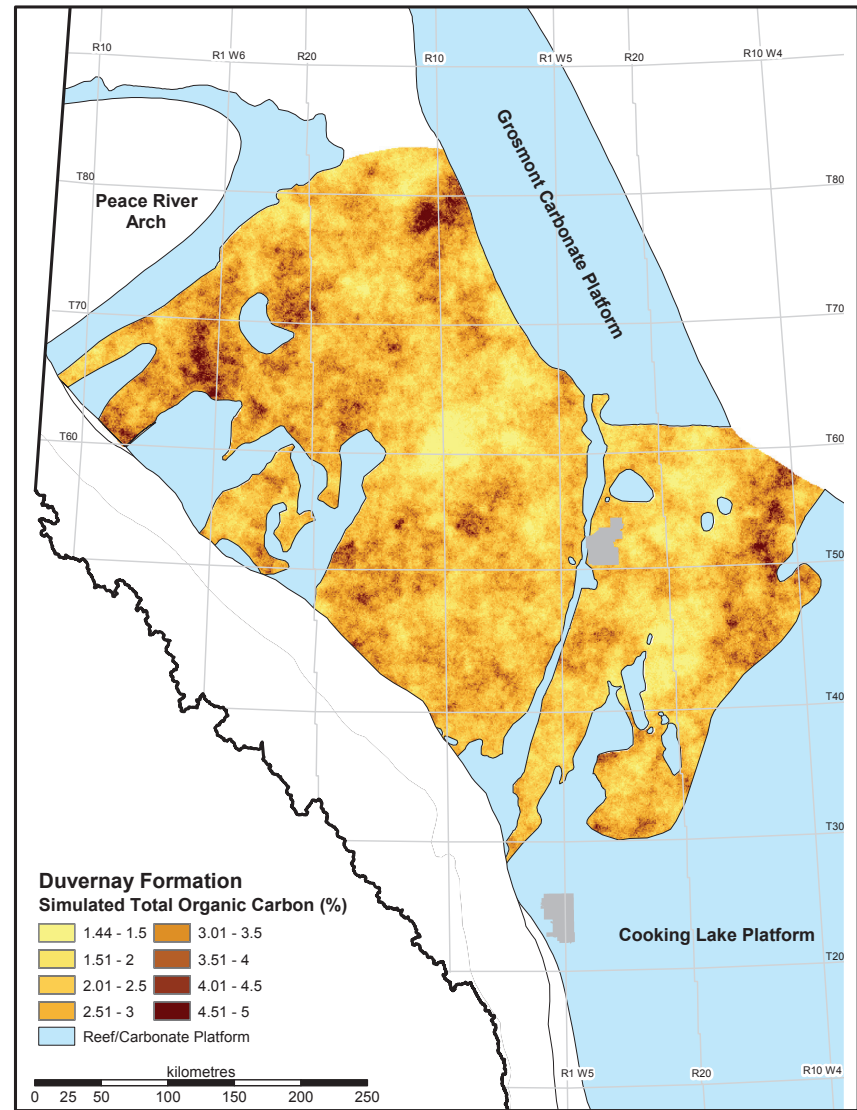
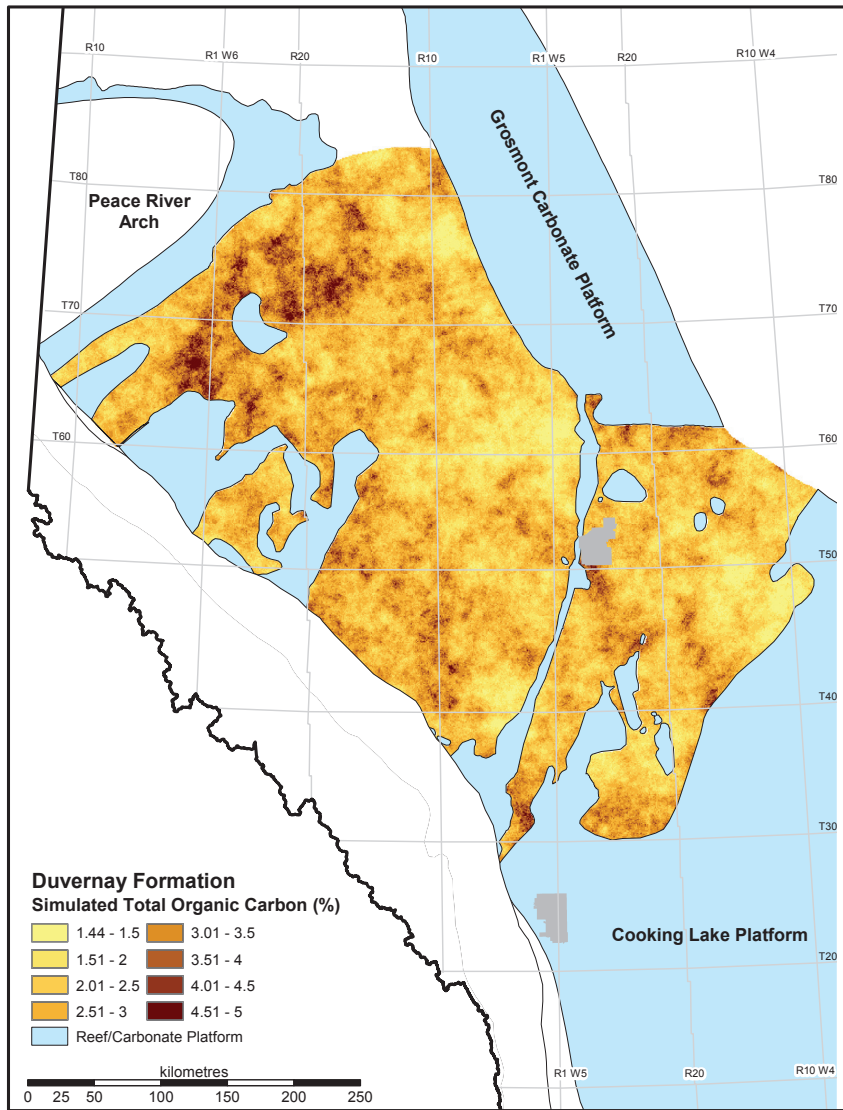


Figure 12. Two realizations of the TOC content of the Duvernay Formation.

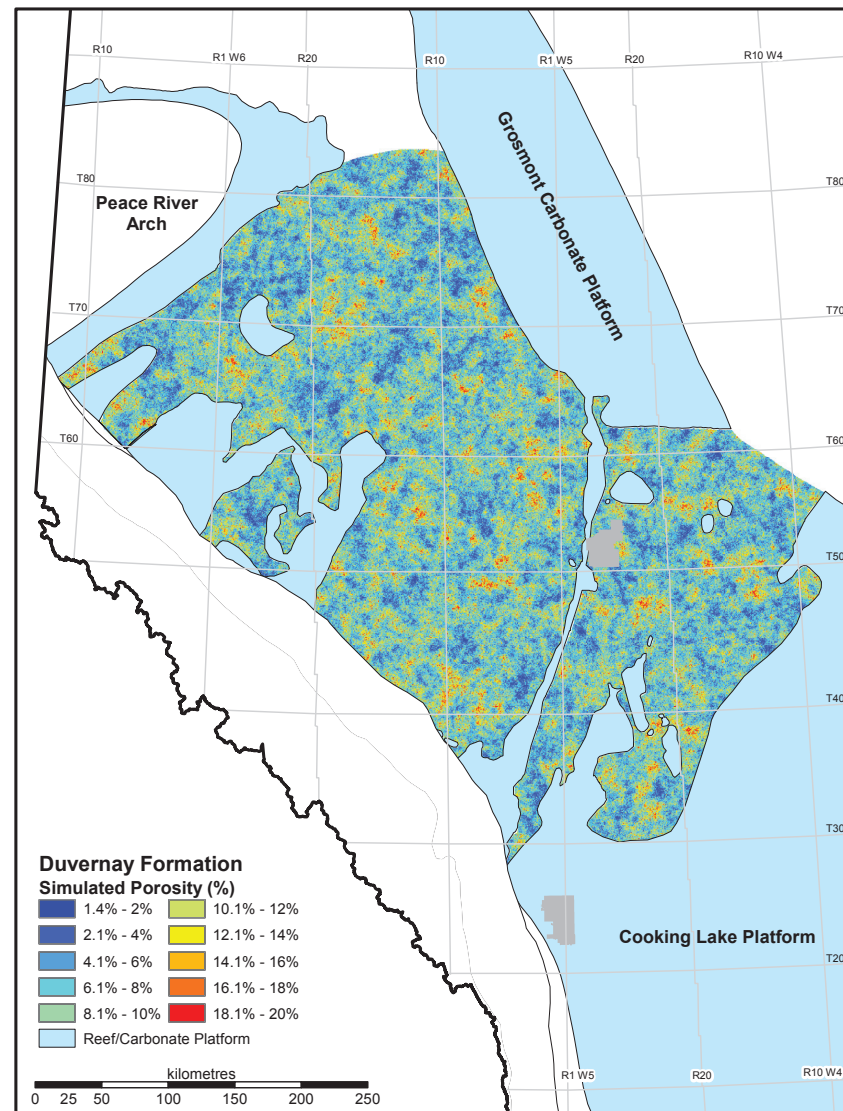
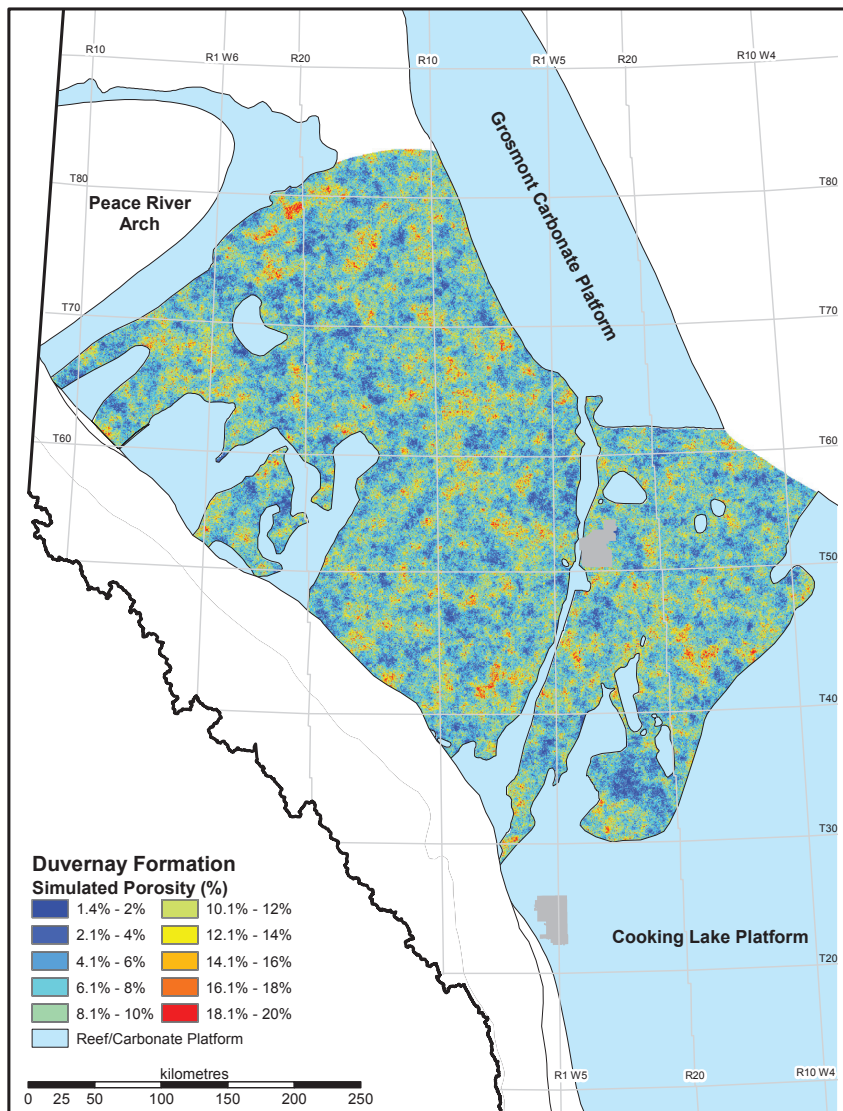


Figure 13. Two realizations of the shale porosity of the Duvernay Formation.

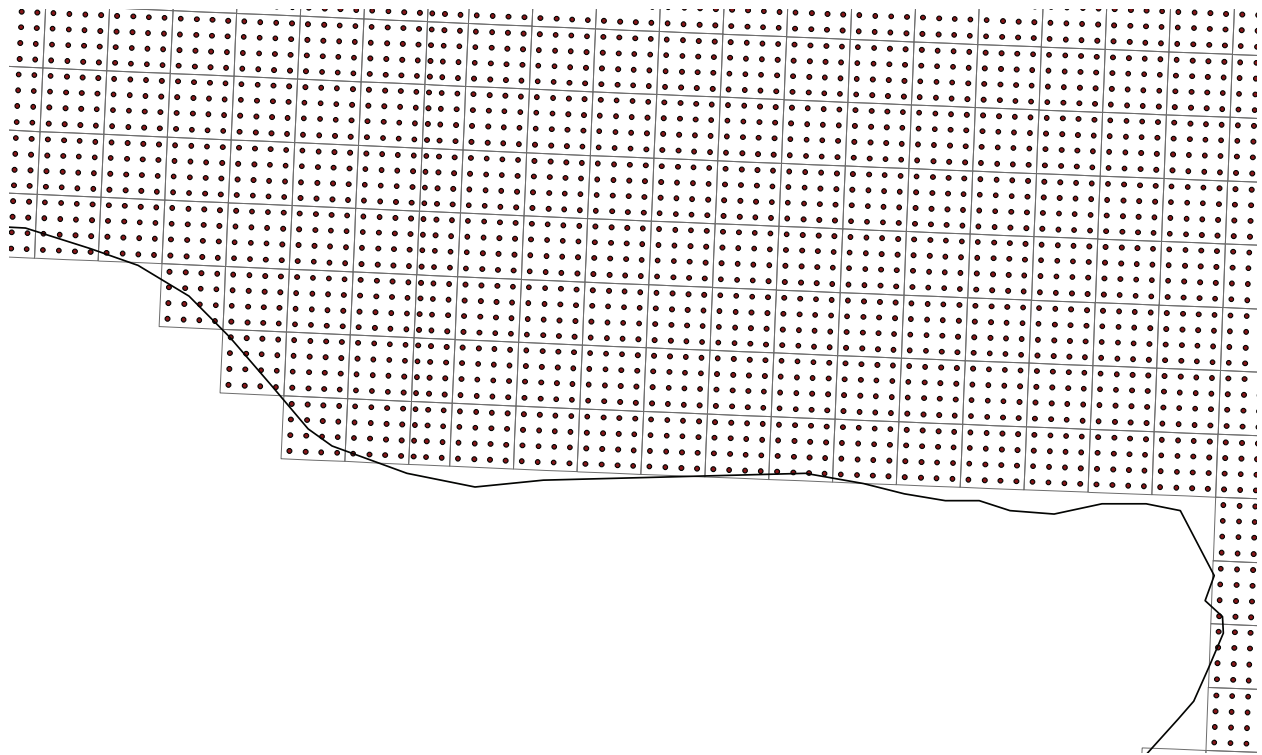


Figure 14. Example of upscaling. The dots are the centroid locations of Alberta Township System Legal Subdivisions on an approximately 400 m grid; the squares are the boundaries of ATS sections that are being evaluated; the dark line is the erosional edge of the shale formation under consideration.

3 Calculating Dependent Variables

Some variables that are needed for resource calculations do not have sufficient data density for direct mapping. Consider the Langmuir isotherm parameters for determining adsorbed gas content, which are found by running isotherm lab analyses. These variables cannot be quickly or easily obtained, and so are quite limited. Other variables, such as reservoir temperature and pressure, are not associated with precise locations or are taken from other formations as analogue data and so the x,y coordinates are not representative of where the value actually occurs in space. These variables are, however, dependent on one or more of the spatial variables.

3.1 Linear Bivariate Relationships

A linear bivariate relationship between two variables has the form

$$Y = X \cdot \beta_1 + \beta_0 \quad (14)$$

where Y is the dependent variable, X is the known (predictive or primary) variable, β_1 is the slope, and β_0 is the intercept.

3.2 Least-Squares Regression

The β parameters in the linear equation are unknown and must be estimated from the available data. This is done by a procedure called linear regression (Ryan, 1997). The slope is estimated by the equation

$$\hat{\beta}_1 = \frac{S_{xy}}{S_{xx}} \quad (15)$$

where $\hat{\beta}_1$ is the estimated slope, S_{xx} is the centred sum of squares for the X variable:

$$S_{xx} = \sum (X - \bar{X})^2 \quad (16)$$

and S_{xy} is the centred sum of products of X and Y :

$$S_{xy} = \sum (X - \bar{X}) \cdot (Y - \bar{Y}) \quad (17)$$

With the slope estimated, the intercept is found by using the slope and means of the variables:

$$\hat{\beta}_0 = \bar{Y} - \hat{\beta}_1 \cdot \bar{X} \quad (18)$$

The parameters found through linear regression give the best-fit line through the x,y data. Figure 15 on page 23 shows the relationship between depth and pressure in the basal Banff/Exshaw shale with the best-fit line. There are some outliers, but in general the points closely follow the regression fit line.

3.3 Regression Uncertainty

The linear regression best-fit line is calculated from sample data, so there is uncertainty associated with it. A number of different relationships can be used to quantify the uncertainty. (See Ryan [1997] for more details.) Note that some of the equations in this section have been rearranged to make them easier to calculate. The uncertainty in the slope and intercept can be found by using the equations

$$S_{\hat{\beta}_1}^2 = \frac{S_e^2}{S_{xx}} \quad (19)$$

$$S_{\hat{\beta}_0}^2 = S_e^2 \cdot \frac{\sum X^2}{n \cdot S_{xx}} \quad (20)$$

where $S_{\hat{\beta}_1}^2$ is the variance of the estimated slope, $S_{\hat{\beta}_0}^2$ is the variance of the estimated intercept, and S_e^2 is the variance of the random fluctuations of the Y data about the estimated linear relationship:

$$S_e^2 = (1 - R^2) \cdot \left(\frac{S_{yy}}{n - 2} \right) \quad (21)$$

where R^2 is the square of the correlation coefficient between the two variables and is a measure of the ‘goodness of fit’ of the linear regression:

$$R^2 = \frac{S_{xy}^2}{S_{xx} \cdot S_{yy}} \quad (22)$$

and S_{yy} is the centred sum of squares of variable Y :

$$S_{yy} = \sum (Y - \bar{Y})^2 \quad (23)$$

3.4 Conditional Uncertainty

The uncertainty in the individual linear regression parameters is calculated from the equations in Section 3.3. However, the slope and intercept are not independent of one another. They are correlated with a correlation coefficient of

$$\rho_{\hat{\beta}_0, \hat{\beta}_1} = - \frac{\sum X}{\sqrt{n \cdot \sum X^2}} \quad (24)$$

where $\rho_{\hat{\beta}_0, \hat{\beta}_1}$ is the correlation coefficient and n is the number of bivariate data. Similar to the difference between local and global uncertainty discussed in Section 2.2, the relationship between slope and intercept must be accounted for through simulation. This can be done by drawing a simulated slope from a t-distribution:

$$\hat{\beta}_1^{sim} \sim t_{n-2}(\hat{\beta}_1, S_{\hat{\beta}_1}^2) \quad (25)$$

where $\hat{\beta}_1^{sim}$ is the simulated slope value, $\hat{\beta}_1$ is the estimated slope, and $S_{\hat{\beta}_1}^2$ is the estimated variance of the slope. The simulated slope is taken from a t-distribution with $n-2$ degrees of freedom. A t-distribution is used rather than a normal distribution because the slope and slope variance are estimated and therefore uncertain (i.e., there is uncertainty in the uncertainty). With a simulated slope value, a simulated intercept conditional to the simulated slope can then be determined:

$$\hat{\beta}_0^{sim} \sim t_{n-2} \left(\hat{\beta}_0 + \frac{S_{\hat{\beta}_0}}{S_{\hat{\beta}_1}} \cdot \rho_{\hat{\beta}_0, \hat{\beta}_1} \cdot (\hat{\beta}_1^{sim} - \hat{\beta}_1), \left(1 - \rho_{\hat{\beta}_0, \hat{\beta}_1}^2 \right) \cdot S_{\hat{\beta}_0}^2 \right) \quad (26)$$

The simulated intercept $\hat{\beta}_0^{sim}$ is drawn from a t-distribution with $n-2$ degrees of freedom and conditional mean and variance as shown above. If the simulated slope is exactly equal to the estimated slope, then the mean of the simulated intercept will be exactly the estimated intercept. Figure 16 shows an example of simulated linear relationships for adsorption isotherm data in the Duvernay Formation. The dark black line is the best-fit line from linear regression, and the coloured lines are simulated realizations of the relationship, each with its own simulated slope and an intercept conditional to that slope. The data points are modified from Beaton et al., 2010a, and Rokosh et al., 2013.

3.5 Bilinear Relationships

Not all bivariate relationships are linear. In the data used for shale gas resource assessment in Rokosh et al. (2012), several of the data sets were found to have bilinear relationships, or linear relationships with an inflection point at which the slope changes. Temperature-depth and pressure-gas compressibility are two bivariate data types that showed a bilinear form in several cases. The equation for this type of relationship is

$$Y = (X - X_{defl}) \cdot (X > X_{defl}) \cdot \beta_2 + X \cdot \beta_1 + \beta_0 \quad (27)$$

where X_{defl} is the value of X at which the deflection point occurs and β_2 is the change in slope from the left of the inflection point to the right of it. Figure 17 shows an example of this type of relationship in the basal Banff/Exshaw shale.

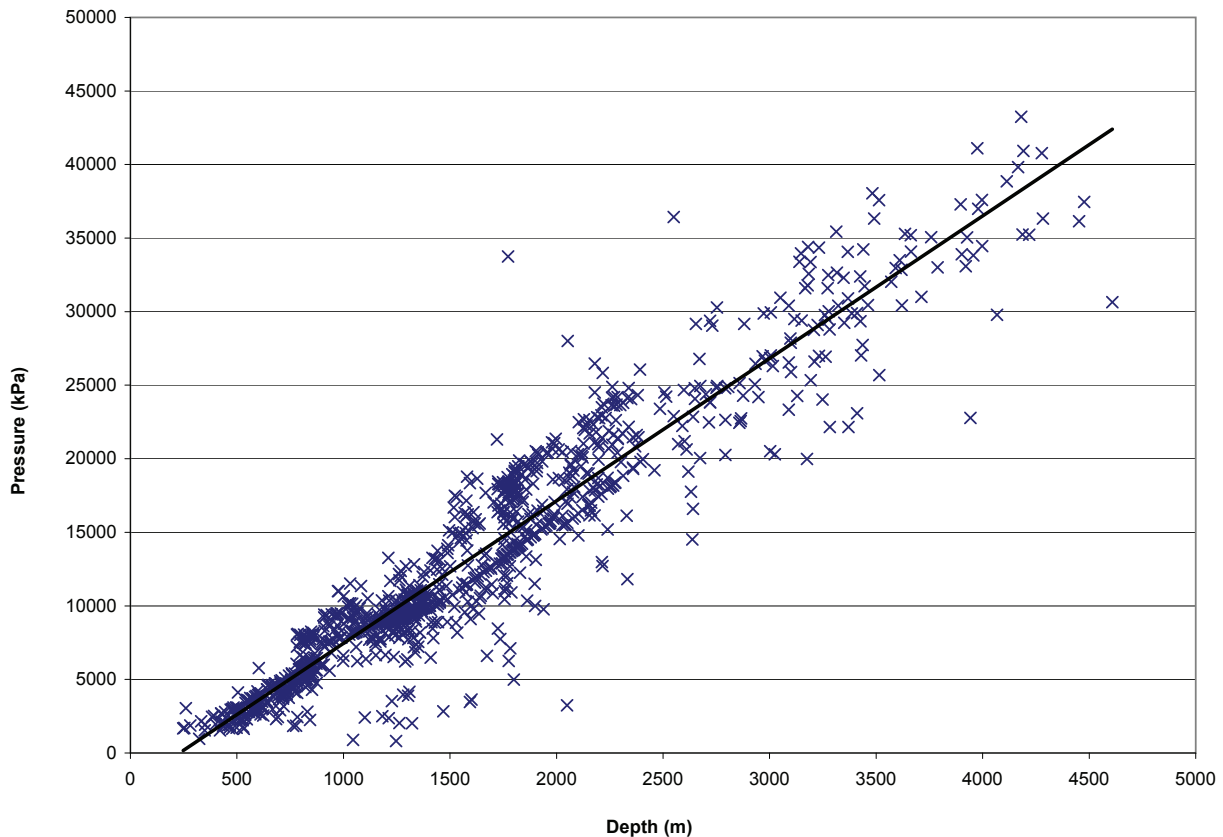


Figure 15. Data showing the pressure vs. gas compressibility relationship in the basal Banff/Exshaw shale (unpublished data).

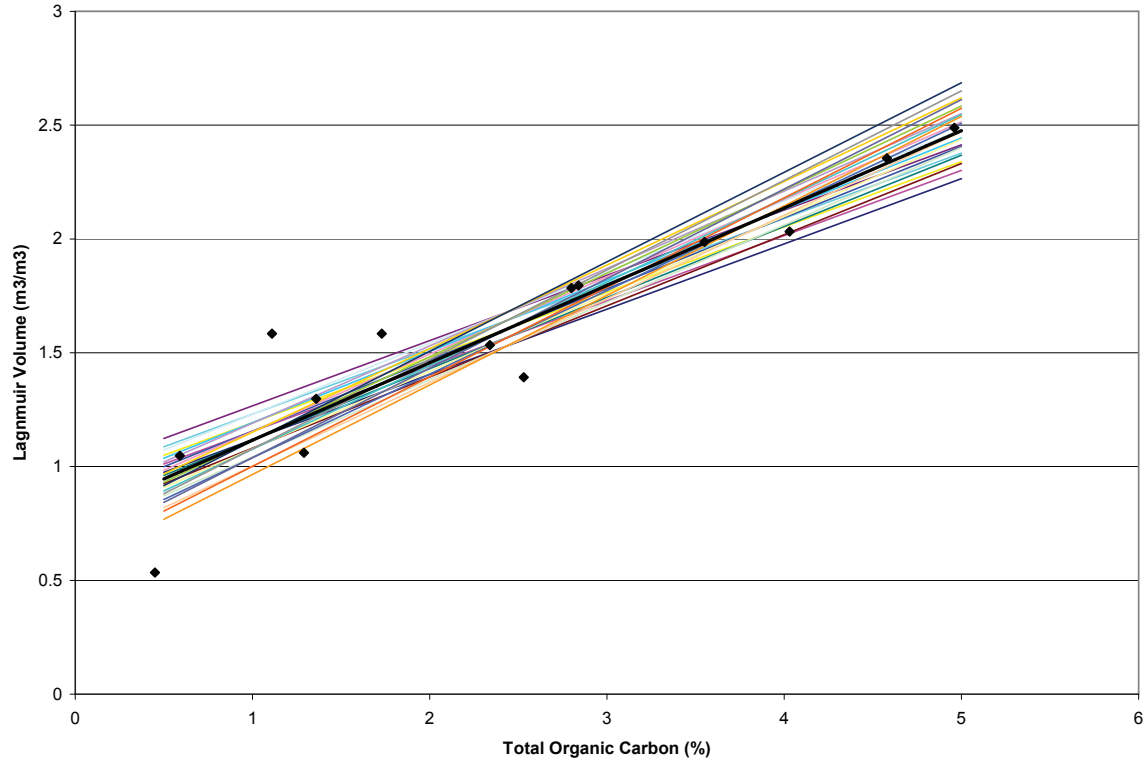


Figure 16. Data showing the uncertainty in the TOC-VL relationship in the Duvernay Formation (data from Beaton et al., 2010a, and Rokosh et al., 2013a). Each coloured line is a simulated realization of the linear regression.

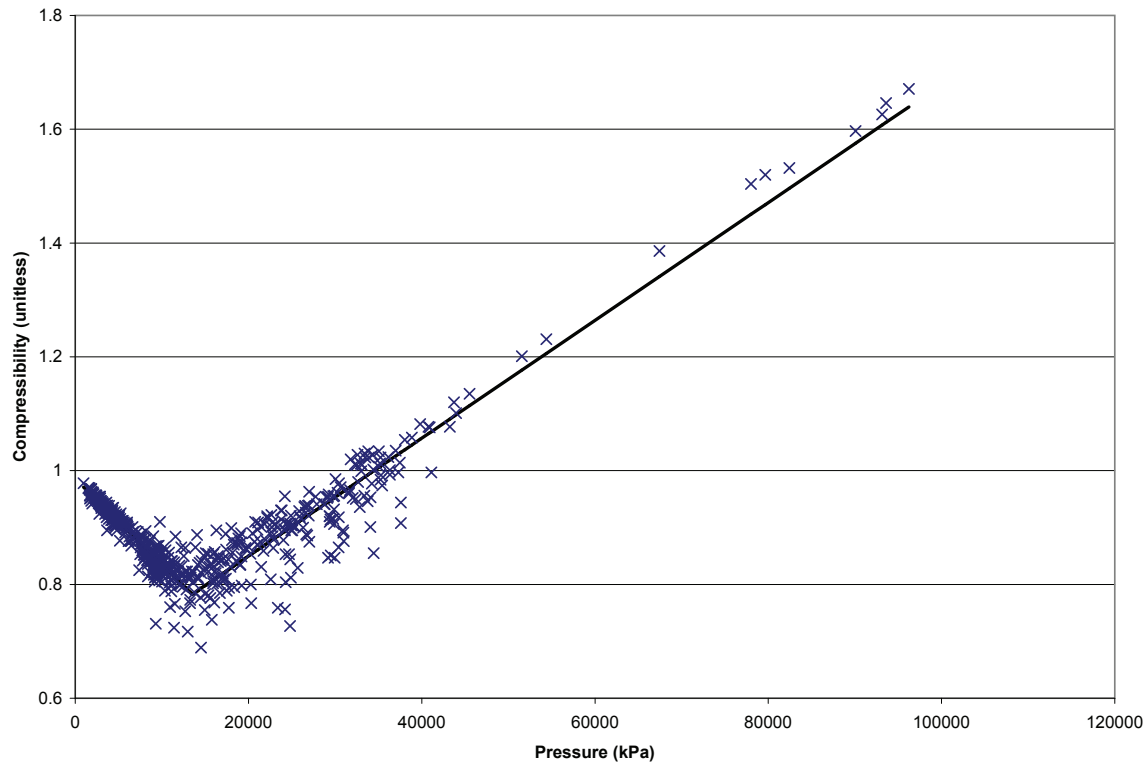


Figure 17. Data showing the pressure vs. gas compressibility relationship in the basal Banff/ Exshaw shale (unpublished data).

4 Determining Other Variables

Some variables that are necessary for shale gas resource evaluation are too limited to be spatially mappable and do not show a significant relationship to other variables, are sampled too sparsely to determine a bivariate relationship, or are determined from lab analyses that were designed for conventional reservoirs and are potentially unreliable in shale, increasing the uncertainty. These variables must be accounted for in the resource assessment. The only way to accomplish this is to determine a value to use at all locations in the resource calculations and apply a distribution of uncertainty.

4.1 Univariate Distributions

A distribution considered by itself and unrelated to another variable is called a univariate distribution. A univariate distribution can be visualized by a histogram and summarized by statistics such as the mean, variance, median, and various quantiles or percentiles.

A univariate distribution is applied to the resource estimates by randomly selecting a single value from the distribution and using that value for all of the resource calculations over the entire area. This is combined with the simulated results for the spatial and dependent variables to quantify the uncertainty in the resources. The distribution that is used should be representative of the mean value of the variable—for example, the expected average water saturation over the entire study area. The uncertainty in the mean can be quantified from the sample distribution by simple statistics or more sophisticated methods such as the bootstrap (Deutsch, 2002).

In practice, the samples for these variables are too limited to quantify the uncertainty in the mean with any confidence. The sample distribution, information released by industry, and experience from analogous formations are combined to determine one distribution that is modelled with the shape of a normal distribution, lognormal distribution, triangular distribution, or another distribution as necessary. The high and low (P10 and P90) quantiles are used to fit the endpoints of the distributions because these are easier to reliably estimate than assuming the mean or median (Rose, 2001). The distributions are fit by expert judgement in answering the question, “What is the highest and lowest value for this variable that I would accept without arguing?” The high and low quantiles can be used to determine the parameters for the chosen distribution shape, and the extreme endpoints (P1 and P99, or even P0.1 and P99.9) are checked to ensure they are in agreement with physical reality—that is, water saturation is bounded by 0% and 100% even in the most extreme cases.

4.1.1 Water Saturation

Water saturation is relatively difficult to determine in shale. Dean Stark analysis provides saturation values but may not be reliable and is too expensive and time consuming to sample extensively. Log analysis derivation of water saturation is a difficult process and may not use standard methods in non-Archie reservoirs such as shale (Worthington, 2011). Furthermore, to our knowledge, the reliability of the estimates has not been verified with lab analysis data. Some information is available from industry releases, and other shale formations that have been evaluated previously by agencies such as the U.S. Geological Survey or others (Faraj et al., 2004; Nieto et al., 2009).

Figure 18 shows water saturation for the Duvernay Formation, as determined by Dean Stark analysis. From this distribution and other available information, a lognormal distribution was used to represent the water saturation in the Duvernay Formation with a low (P10) value of 10%, a high (P90) value of 30%, and a resulting median (P50) value of 17.3% and mean of 19%. The minimum and maximum values from simulation are 4% and 77%, representing the most extreme cases in a best-case or worst-case scenario, respectively.

4.1.2 Grain Density

The grain density as determined from mineralogy has a significant impact on the porosity in tight reservoirs, including shale formations (Rokosh et al., 2010). Small variations in grain density have a greater relative impact on estimated porosity when there is less pore space. Porosity is calculated from density logs by using the equation

$$\phi = \frac{\rho_g - \rho_b}{\rho_g - \rho_f} \quad (28)$$

where ϕ is the porosity, ρ_g is the grain density, ρ_b is the log bulk density, and ρ_f is the fluid density. Setting the bulk density as a known value and rearranging the equation for multiple grain densities results in the following equation:

$$\phi' = \frac{\rho'_g - \rho_g + \phi \cdot (\rho_g - \rho_f)}{\rho'_g - \rho_f} \quad (29)$$

where ϕ' is the modified porosity for a new grain density ρ'_g . This allows the log density porosity to be calculated and modelled then modified to account for uncertainty in the grain density.

Figure 19 shows a histogram of the grain density in the Duvernay Formation (Anderson et al., 2010). From this data and other sources, a range of grain density of 2.64 g/cm³ to 2.70 g/cm³ was determined to be appropriate with a normal distribution shape. This was modelled using a normal distribution with a mean of 2.67 g/cm³ and a standard deviation of 0.025 g/cm³. The minimum to maximum values from simulation range from 2.59 to 2.76 g/cm³. The presence of TOC in shale must be taken into account before determining total porosity from log analysis by treating TOC as another mineral contributing to the grain density.

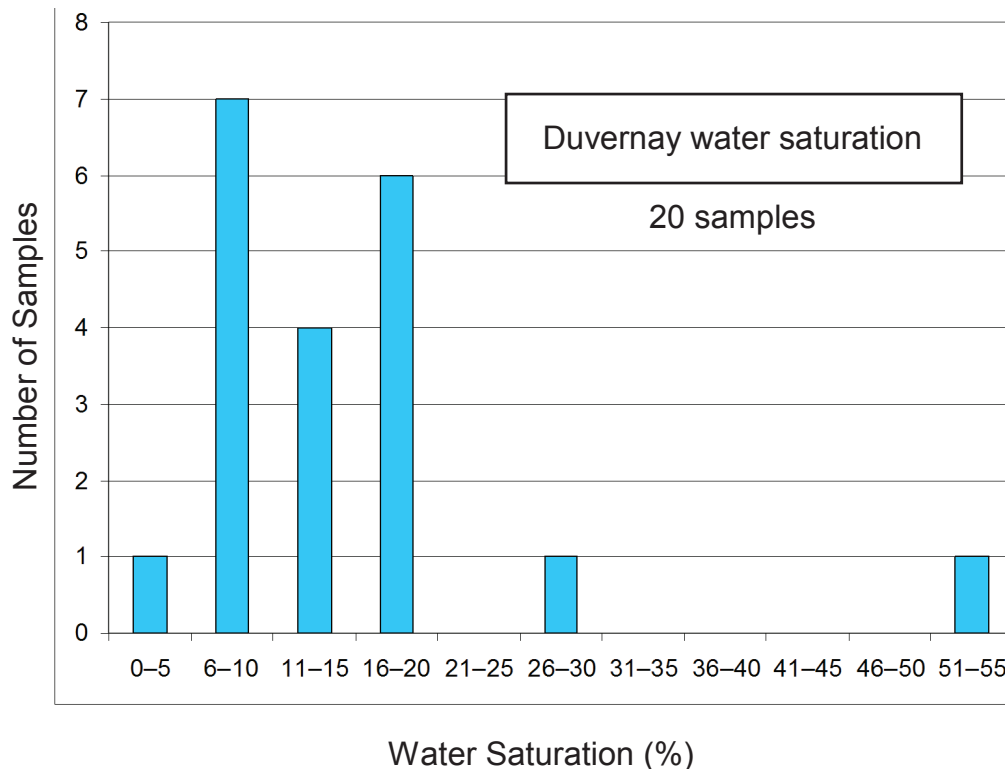


Figure 18. Histogram of water saturation, determined by Dean Stark analysis, in the Duvernay Formation (Rokosh et al., 2012).

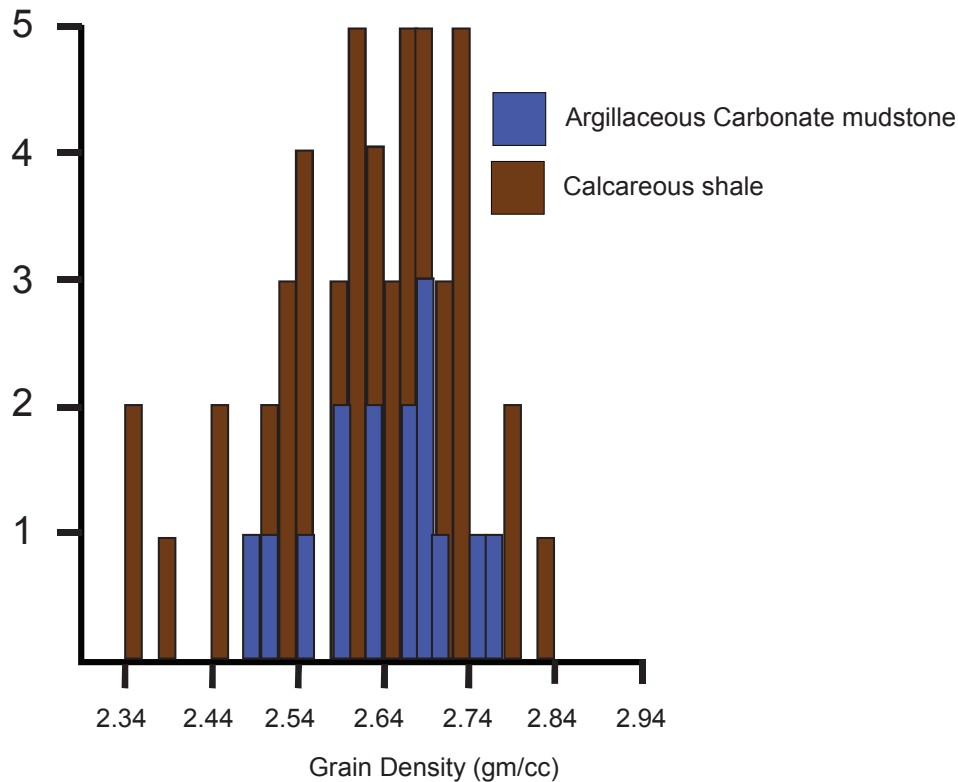


Figure 19. Histogram of grain density in the Duvernay Formation (from Anderson et al., 2010).

5 Fluid Zones

Shale formations span vast areas and wide ranges of burial depths and thermal maturities. During the burial history of many shale formations in the Western Canada Sedimentary Basin (WCSB), kerogen has been converted into oil and gas. These different fluids occurred in different zones over the span of an entire shale formation and existed simultaneously at different locations. To account for gas, oil, and intermediate hydrocarbons, maturity maps were created to determine the fluid distribution.

5.1 Maturity Maps

The primary variables used to determine thermal maturity are vitrinite reflectance and Tmax. Other indicators of fluid makeup, such as hydrogen index or production index, can prove useful. These variables are mapped as spatial variables if sample density is sufficient; otherwise, a bivariate relationship with depth should be useful. The mapping method used in this particular case for some formations evaluated in Rokosh et al. (2012) was cokriging, with depth as a secondary variable. Figure 20 on page 31 shows a map of vitrinite reflectance and hydrogen index in the Duvernay Formation. Spatial simulation was not possible in these early assessments due to a lack of data. Uncertainty is accounted for by varying the zone cutoffs, as discussed below.

5.2 Zone Cutoffs

With the maturity variables mapped, the zones containing different fluids need to be determined. Table 2 shows the six zones that are used in this methodology for fluid content, from Danesh (1998), as well as the assigned range of gas-oil ratio (GOR) and vitrinite reflectance (modified from Peters and Casa [1994] and Baskin [1997]). Other variables (Tmax, HI, etc.) could be used with a similar cutoff scheme.

Table 2. Duvernay vitrinite reflectance (left) and hydrogen index (right) (Rokosh et al., 2012).

Zone	Gas-Oil Ratio (m ³ /m ³)	Vitrinite Reflectance (% Ro)
Dry Gas	Infinity (i.e., no oil)	>1.35
Wet Gas	Infinity (i.e., no oil)	1.20–1.35
Condensate	570–10 000	1.00–1.20
Volatile (Gassy) Oil	310–570	0.85–1.00
Black Oil	0–310	0.80–0.85
Immature	0 (i.e., no gas)	<0.80

The uncertainty in the zone definitions is accounted for by varying the zone cutoffs as univariate variables (see Section 4). By taking this approach, only one map of maturity needs to be constructed, and the zones vary smoothly based on the cutoffs that are simulated. The distribution of the cutoffs is chosen by looking at the magnitude of misclassifications between the map and the data. A typical range for the shale appraisals in Rokosh et al. (2012) was to vary the cutoffs by a factor of 0.75 to 1.25 with a triangular distribution.

5.3 Saturations and Coproduct Ratios

Once the zones are defined, the GOR is defined at the boundaries between zones. The coproduct (condensate-gas) ratio (CGR) also needs to be defined. To determine the CGR, available gas tests in analogue formations or adjacent zones are used:

$$CGR \left[\frac{m^3}{e^3 m^3} \right] = \left(C_2 \cdot \frac{0.65}{281.3} + C_3 \cdot \frac{0.85}{272.3} + C_4 \cdot \frac{0.90}{234.5} + C_{5+} \cdot \frac{1.0}{182.0} \right) \cdot 1000 \quad (30)$$

where C_2 , C_3 , C_4 , and C_{5+} represent different hydrocarbons from the gas test data. These results are combined with industry data from early wells (Penty, 2011) to determine the maximum CGR (which would exist at the boundary between the condensate and volatile oil zones) and an intermediate CGR value (at the boundary between the condensate and wet gas zones).

5.3.1 Linear Interpolation

With the GOR and CGR values determined for the zone boundaries, values are assigned to individual locations. This is done by linear interpolation based on the maturity map:

$$GOR = MINGOR + \frac{MAXGOR - MINGOR}{MAXRO - MINRO} \cdot (RO - MINRO) \quad (31)$$

where $MINGOR$ and $MAXGOR$ are the minimum and maximum GORs in the fluid zone, $MINRO$ and $MAXRO$ are the zone boundary vitrinite reflectance cutoff values, RO is the mapped vitrinite reflectance, and GOR is the modelled GOR. The CGR is found using the same approach:

$$CGR = MAXCGR - \frac{MAXCGR - MINCGR}{MAXRO - MINRO} \cdot (RO - MINRO) \quad (32)$$

where $MINCGR$ and $MAXCGR$ are the minimum and maximum condensate-gas ratios in the fluid zone.

5.3.2 Calculating Saturations

The GOR can be expressed as the volumetric ratio between gas and oil in the formation, with the gas and oil contents expanded to their constituent volumetric parameters:

$$GOR = \frac{GIP_{free}}{OIP} = \frac{AREA \cdot NET \cdot PHI \cdot SG \cdot \frac{PRES}{101} \cdot \frac{288}{TEMP} \cdot \frac{1}{ZI}}{AREA \cdot NET \cdot PHI \cdot SO \cdot \frac{1}{BOI}} \quad (33)$$

This can be rearranged and combined with water saturation, and the identity $S_g + S_o + S_w = 1$, to solve for the unknown gas and oil saturations:

$$SG = (1 - SW) \cdot \frac{GOR \cdot \frac{TEMP}{288} \cdot \frac{101}{PRES} \cdot \frac{ZI}{BOI}}{GOR \cdot \frac{TEMP}{288} \cdot \frac{101}{PRES} \cdot \frac{ZI}{BOI} + 1} \quad (34)$$

$$SO = 1 - SW - SG \quad (35)$$

The gas and oil saturations are now defined for all locations and can be used in resource calculations.

6 Resource Calculations

The methodology presented here uses a volumetric approach to calculating resources. The quantity of free gas in a volume of rock at reservoir conditions is calculated as follows:

$$GIP_{free} = AREA \cdot NET \cdot PHI \cdot SG \cdot \frac{PRES}{101} \cdot \frac{288}{TEMP} \cdot \frac{1}{ZI} \quad (36)$$

The area used in this methodology could be any size, but as in Section 2.3, the unit area is an ATS section, or 1 square mile (1609 m by 1609 m). Care must be taken to balance the units in volumetric equations to obtain results in the desired system of measurement. The quantity of adsorbed gas in a reservoir is calculated as:

$$GIP_{ads} = AREA \cdot NET \cdot \frac{VL}{(PRES + PL)} \quad (37)$$

Adsorbed gas still increases with pressure as more gas is forced into the same volume of rock, but by a different mechanism than free gas. The total gas in place is then

$$GIP_{tot} = GIP_{free} + GIP_{ads} \quad (38)$$

The volume of natural gas liquids (condensate) is calculated by using the coproduct ratio:

$$NGLIP = GIP_{free} \cdot CGR \quad (39)$$

Oil in place is a volumetric calculation similar to the free gas in place equation:

$$OIP = AREA \cdot NET \cdot PHI \cdot SO \cdot \frac{1}{BOI} \quad (40)$$

The reservoir parameters are different than for gas, but the calculation is essentially pore space multiplied by saturation.

Once the resources have been calculated for every section in the study area, the results can be summarized as needed. Summing the resources in every section gives the total resources in the study area; mapping section-by-section resources produces a map of hydrocarbons in place. It is recommended that the hydrocarbon quantities not be mapped at such a fine scale as a section so that overinterpretation is not an issue. Rokosh et al. (2012) summarized shale- and siltstone-hosted hydrocarbon resources in Alberta at the township (six sections by six sections) scale.

7 Simulation and Joint Uncertainty

The uncertainty in individual variables can be quantified by maps, bivariate scatterplots, or histograms. However, when taken together, the distribution of all variables simultaneously is too complex to summarize in any simplified way. Every parameter used in the equations in Section 6 is a variable with uncertainty. Combining these variables in nonlinear equations produces results that cannot be explicitly defined in a theoretical way; the distribution of the output (i.e., the resource numbers) is not a well-defined parametric distribution. The volumetric resource calculations can be viewed as a transfer function—that is, a set of equations that take a set of input parameters and produce a single output for each unique input. By varying the input parameters through simulation, a number of output values can be obtained. The resulting output is a representative sample of the distribution of uncertainty of the output variable. The methodology presented in this report has been constructed to produce distributions for every parameter to work towards simulation of the hydrocarbon resources in shale reservoirs. Repeating the simulation procedure many times (1000 or more) produces an estimate of the resources and uncertainty at all locations and in any desired subareas. The resources are usually summarized by P10, P50, and P90 values for a defined area, which could be the entire shale formation, a study or play area, townships, map sheets, municipalities, or any other geographic distribution. Figure 21 shows maps of the hydrocarbon resources in the shale portion of the Duvernay Formation. The resources were calculated at the section scale but are summarized at the township scale in Figure 21. Figure 22 shows a conceptual diagram of the transfer function for the methodology presented in this report.

8 Conclusions

The methodology presented in this report is to calculate shale and other continuous unconventional resources for which few wells are available for data collection and little or no production history is established. The methodology has proven to be robust regarding data availability to determine resource endowment for a formation and also to identify areas where land sales and drilling may first occur. The latter is useful for planning by local and provincial governments and agencies.

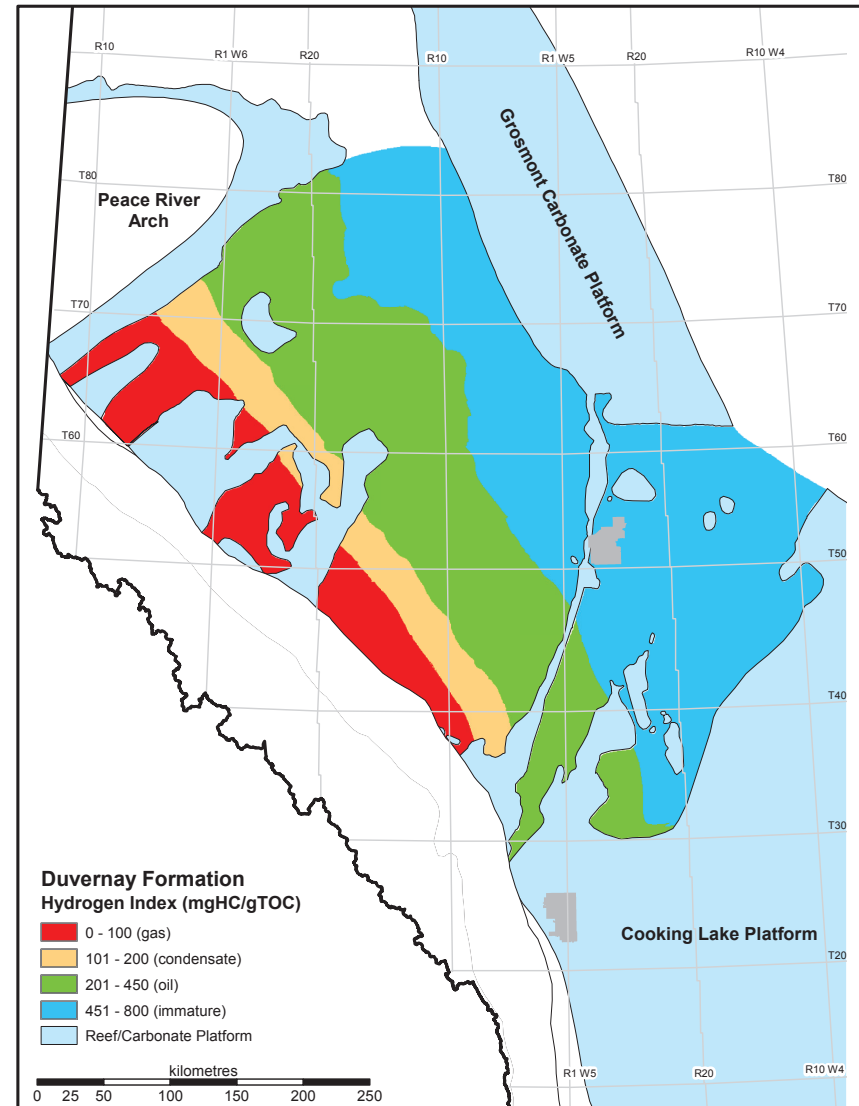
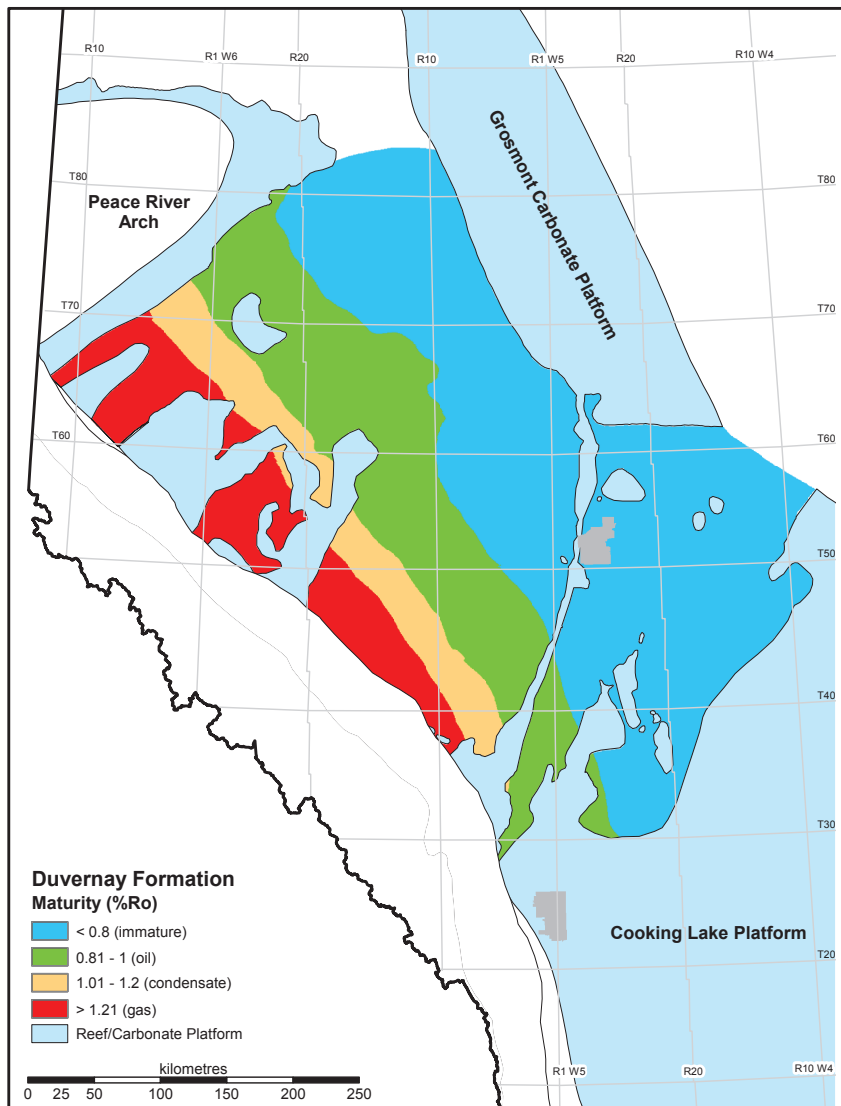


Figure 20. Duvernay vitrinite reflectance (left) and hydrogen index (right) (Rokosh et al., 2012).

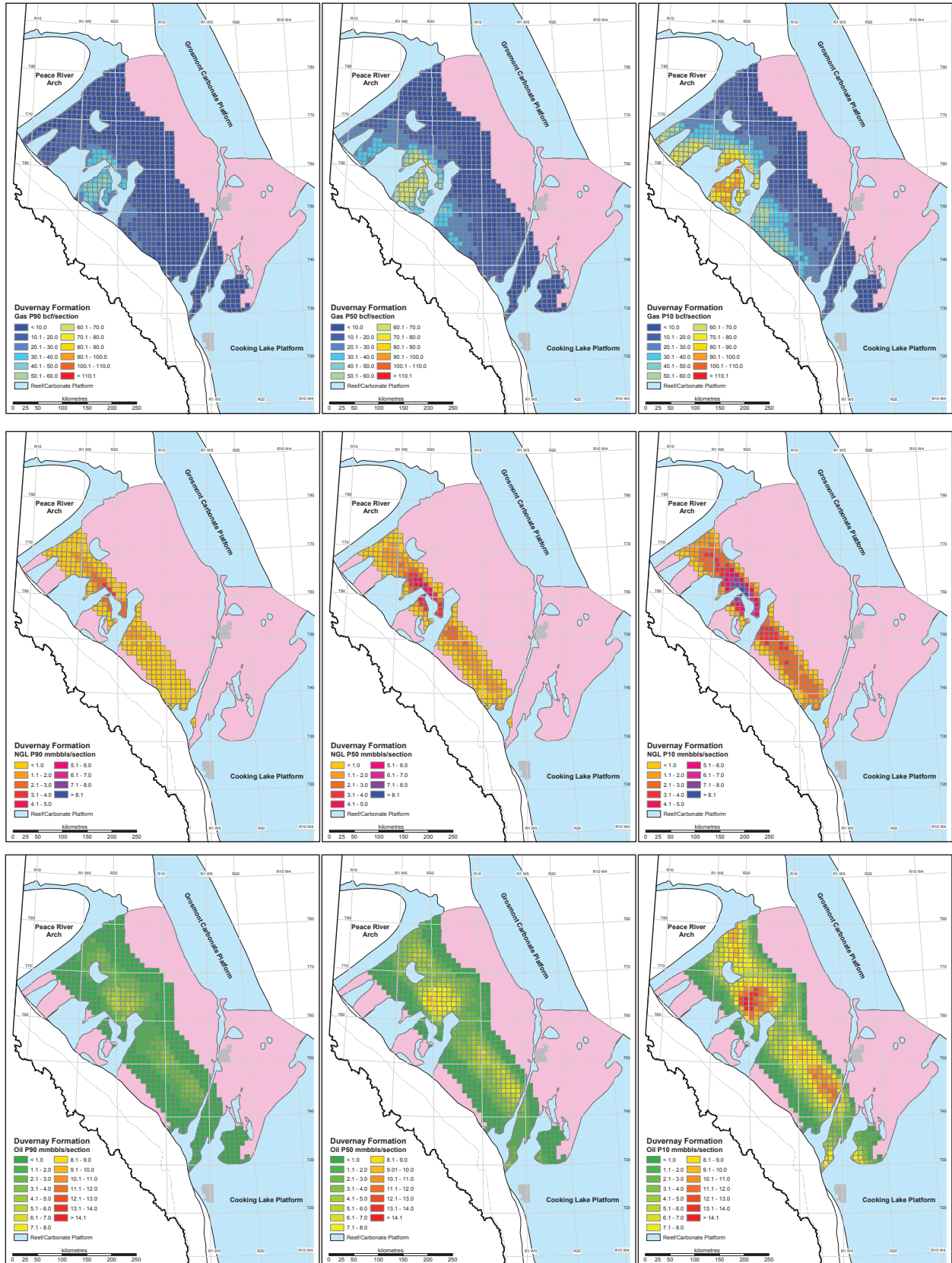


Figure 21. Shale resource maps for the Duvernay Formation (Rokosh et al., 2012).

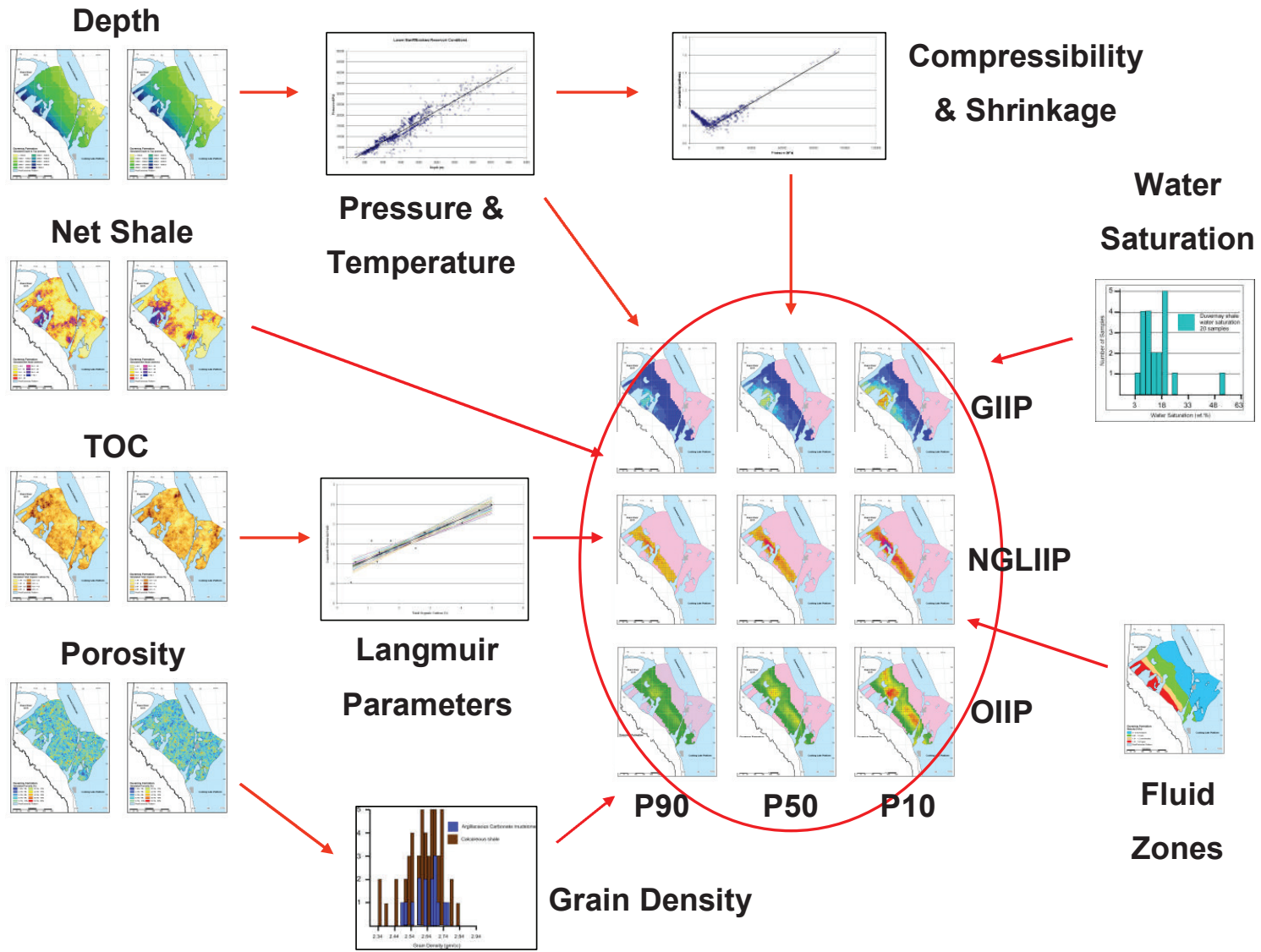


Figure 22. Conceptual diagram of the transfer function for the quantification of uncertainty in shale resources.

9 References

- Anderson, S.D.A., Beaton, A.P., Berhane, H., Pawlowicz, J.G. and Rokosh, C.D. (2010): Mineralogy, permeametry, mercury porosimetry, pycnometry and scanning electron microscope imaging of Duvernay and Muskwa formations: Shale gas data release; Energy Resources Conservation Board, ERCB/AGS Open File Report 2010-02, 67 p.
- Baskin, D.K. (1997): Atomic H/C ratio of kerogen as an estimate of thermal maturity and organic matter conversion; American Association of Petroleum Geologists Bulletin, v. 81, no. 9, p. 1437–1450.
- Beaton, A.P., Pawlowicz, J.G., Anderson, S.D.A., Berhane, H. and Rokosh, C.D. (2010a): Rock Eval™, total organic carbon and adsorption isotherms of the Duvernay and Muskwa formations in Alberta: shale gas data release; Energy Resources Conservation Board, ERCB/AGS Open File Report 2010-04, 33 p.
- Beaton, A.P., Pawlowicz, J.G., Anderson, S.D.A., Berhane, H. and Rokosh, C.D. (2010b): Organic petrography of the Duvernay and Muskwa formations in Alberta: shale gas data release; Energy Resources Conservation Board, ERCB/AGS Open File Report 2010-06, 147 p.
- Chiles, J.P. and Delfiner, P. (2012): Geostatistics: modeling spatial uncertainty (2nd edition); Wiley, New York, New York, 734 p.
- Danesh, A. (1998): PVT and phase behaviour of petroleum reservoir fluids; Elsevier Science B.V., London, UK, 388 p.
- Deutsch, C.V. (2002): Geostatistical reservoir modeling; Oxford University Press, New York, New York, 376 p.
- Everett, R.V. (2011): Log and core TOC in three formations (Muskwa, Duvernay, Montney); unpublished presentation prepared by Robert V. Everett Petrophysics Inc. for the Energy Resources Conservation Board.
- Faraj, B. (2005): Opening remarks from the chair; The Canadian Institute, Capturing Opportunities in Canadian Shale Gas conference, Calgary, AB, January 31–February 1, 2005.
- Faraj, B., Williams, H., Addison, G., Donaleshen, R., Sloan, G., Lee, J., Anderson, T., Leal, R., Anderson, C., Lafleur, C. and Ahlstrom, J. (2002): Gas shale potential of selected Upper Cretaceous, Jurassic, Triassic and Devonian shale formations in the WCSB of Western Canada: implications for shale gas production; report prepared for the Gas Technology Institute, GRI-02/0233, 285 p.
- Faraj, B., Williams, H., Addison, G. and McKinstry, B. (2004): Gas potential of selected shale formations in the Western Canadian Sedimentary Basin; Gap TIPS, v. 10, no. 1, p. 21–15.
- Goovaerts, P. (1997): Geostatistics for natural resources evaluation; Oxford University Press, New York, New York, 483 p.
- Journel, A.G. and Huijbregts, Ch.J. (1978): Mining geostatistics; Academic Press, New York, New York, 600 p.
- McKercher, R.B. and Wolfe, B. (1986): Understanding western Canada's dominion land survey system; Division of Extension and Community Relations, University of Saskatchewan, 26 p.
- Nieto, J., Bercha, R., and Chan, J. (2009): Shale Gas Petrophysics – Montney and Muskwa, are they Barnett Look-Alikes?; Society of Petrophysicists and Well Log Analysts, 50th Annual Logging Symposium, The Woodlands, TX, June 21-24, 2009, p. 30-45.

- Passey, Q. R., Creaney, S., Kulla, J.B., Moretti, F.J. and Stroud, J.D. (1990): A practical model for organic richness from porosity and resistivity logs; American Association of Petroleum Geologists Bulletin, v. 74, no. 12, p. 1777–1794.
- Penty, R. (2011): Encana buys rights in hunt for liquid gas; Postmedia News, June 17, 2011.
- Peters, K.E. and Cassa, M.R. (1994): Applied source rock geochemistry; in The petroleum system: from source to trap, L.B. Magoon and W.G. Dow (ed.), American Association of Petroleum Geologists Memoir 60, p. 93–120.
- Rokosh, C.D., Anderson, S.D.A., Pawlowicz, J.G., Lyster, S., Berhane, H. and Beaton, A.P. (2010): Mineralogy and grain density of Alberta shale; American Association of Petroleum Geologists, Hedberg conference, December 5–10, 2010, Austin, Texas, 1 p.
- Rokosh, C.D., Lyster, S., Anderson, S.D.A., Beaton, A.P., Berhane, H., Brazzoni, T., Chen, D., Cheng, Y., Mack, T., Pana, C. and Pawlowicz, J.G. (2012): Summary of Alberta's shale- and siltstone-hosted hydrocarbon resource potential; Energy Resources Conservation Board, ERCB/AGS Open File Report 2012-06, 327 p.
- Rokosh, C.D., Crocq, C.S., Pawlowicz, J.G. and Brazzoni, T. (2013a): Rock Eval™ and total organic carbon of sedimentary rocks in Alberta (tabular data, tab-delimited format); Energy Resources Conservation Board, ERCB/AGS Digital Dataset 2013-0003, URL <http://www.ags.gov.ab.ca/publications/abstracts/DIG_2013_0003.html> [April 2013].
- Rokosh, C.D., Crocq, C.S., Pawlowicz, J.G. and Brazzoni, T. (2013b): Fluid Saturations of Alberta Geological Units for Shale- and Siltstone-Hosted Hydrocarbon Evaluation (tabular data, tab-delimited format); Energy Resources Conservation Board, ERCB/AGS Digital Dataset 2013-0015, URL <http://ags.gov.ab.ca/publications/abstracts/DIG_2013_0015.html> [May 2013].
- Rose, P.R. (2001): Risk analysis and management of petroleum exploration ventures; American Association of Petroleum Geologists, AAPG Methods in Exploration Series No. 12, 164 p.
- Ryan, T.P. (1997): Modern regression methods; Wiley Interscience, New York, New York, 515 p.
- Schmoker, J.W. (2005): U.S. Geological Survey assessment concepts for continuous petroleum accumulations; in Petroleum systems and geologic assessment of oil and gas in the southwestern Wyoming province, Wyoming, Colorado, and Utah, USGS Southwestern Wyoming Province Assessment Team (ed.), U.S. Geological Survey Digital Data Series DDS-69-D, Chapter 13, 7 p., URL <<http://pubs.usgs.gov/dds/dds-069/dds-069-d/reports.html>> [April 2013].
- Society of Petroleum Evaluation Engineers (Calgary Chapter) (2007): Canadian oil and gas evaluation handbook; Society of Petroleum Evaluation Engineers (Calgary Chapter) and Canadian Institute of Mining, Metallurgy, and Petroleum (Petroleum Society), Calgary, Alberta, 3 volumes.
- Worthington, P.F. (2011): The petrophysics of problematic reservoirs; Journal of Petroleum Technology, v. 63, no. 9, p. 88–97.